


5-2012

Electrospun Polycaprolactone Nanofiber Scaffolds for Tissue Engineering

Andreas Haukas

University of Arkansas, Fayetteville

Follow this and additional works at: <http://scholarworks.uark.edu/etd>

 Part of the [Cell Biology Commons](#), [Molecular, Cellular, and Tissue Engineering Commons](#), and the [Polymer and Organic Materials Commons](#)

Recommended Citation

Haukas, Andreas, "Electrospun Polycaprolactone Nanofiber Scaffolds for Tissue Engineering" (2012). *Theses and Dissertations*. 411.
<http://scholarworks.uark.edu/etd/411>

This Thesis is brought to you for free and open access by ScholarWorks@UARK. It has been accepted for inclusion in Theses and Dissertations by an authorized administrator of ScholarWorks@UARK. For more information, please contact scholar@uark.edu, ccmiddle@uark.edu.

**ELECTROSPUN POLYCAPROLACTONE NANOFIBER SCAFFOLDS
FOR TISSUE ENGINEERING**

**ELECTROSPUN POLYCAPROLACTONE NANOFIBER SCAFFOLDS
FOR TISSUE ENGINEERING**

A thesis submitted in partial fulfillment
of the requirements for the degree of
Master of Science in Biomedical Engineering

By

Andreas Haukas
Oral Roberts University
Bachelor of Science in Biomedical Engineering, 2007

May 2012
University of Arkansas

ABSTRACT

Stem cell and tissue engineering offer us with a unique opportunity to research and develop new therapies for treating various diseases that are otherwise incurable using traditional medicines. However, development of these new therapies relies upon the establishment of *in vitro* cell culture and differentiation systems that mimic *in vivo* microenvironments required for cell-cell and cell-ECM interaction. The development of these cell culture systems depends upon the identification of appropriate biomaterials and cell sources. Biomaterials should be carefully selected and fabricated into scaffolds for supporting cell growth and differentiation. In this study, we explored the fabrication of 3D electrospun nanofiber scaffolds and demonstrated the feasibility of using these scaffolds for supporting cell growth. The material that we used for scaffold fabrication is a polymer, polycaprolactone (PCL). We discovered that the electrospun PCL nanofibers are highly hydrophobic, unsuitable for cell growth. The treatment of PCL electrospun nanofibers with oxygen plasma treatment endowed the fibers with hydrophilic property, making them suitable for cell growth. Our studies suggested that the length of oxygen plasma treatment considerably influences the water contact degree of the nanofibers and their hydrophilicity. The optimization of oxygen plasma treatment resulted in significant improvement of cell proliferation within the electrospun nanofiber scaffolds. Our results provide insight into plasma treatment effects on electrospun PCL as they relate to material properties and cell growth.

This thesis is approved for
recommendation to the
Graduate Council

Thesis Director:

Dr. Kaiming Ye

Thesis Committee:

Dr. Yanbin Li

Dr. Robert Beitle

Dr. Sha Jin

THESIS DUPLICATION RELEASE

I hereby authorize the University of Arkansas Libraries to duplicate this thesis when needed for research and/or scholarship.

Agreed

Andreas Haukas

Refused

Andreas Haukas

ACKNOWLEDGEMENTS

I will start by noting my deepest appreciation for my graduate mentor and advisor, Dr. Kaiming Ye. His continued guidance and patience over the past several years has been irreplaceable, and has allowed me to develop the knowledge and skills to succeed in my research. I will always look fondly on my time spent in the lab and in meetings with him, and will look to replicate his drive and ambition into my future work.

I would also like to express my sincere thanks and gratitude to my thesis committee members, Drs. Sha Jin, Yanbin Li, and Robert Beitle. Their invaluable inputs and considerations have been of great assistance in my studies. A special mention is for Dr. Sha Jin who mentored and advised me. She has been particularly active in the lab, and consistently provided great insight and experimental design considerations throughout the course of my studies. Special thanks go out to Drs. Sreekala Bajwa and Min Zou and Mr. Samuel Beckford, who freely provided their equipment and expertise in my experiments related to material property analysis. Without their assistance and input I would not have been able to provide the complete set of material property data and analysis.

I would also like to thank Mr. Errol Porter, Drs. Jining Xie, Lingfen Chen, and Mourad Benamara. Their assistance in their respective areas of expertise and instrumentation have allowed me to conduct my research and also gain valuable knowledge throughout the process of performing my experimental analysis with their assistance.

My experience and degree would not have been possible if not for the great people in the Engineering Research Center and the Biological and Agricultural Engineering department. A special thank you to Dr. Carl Lewis Griffis, Ms. Linda Pate, Mrs. June and Mr. Mike Brosius,

Mr. Eric den Boer, and all of the staff who have assisted and guided me throughout my studies in the Engineering Research Center.

I am particularly thankful for the wonderful camaraderie amongst my fellow students and researchers within our lab. A big thank you to Dr. Jithesh Veetil, Mr. Karl Sonntag, Miss. Weiwei Wang, Mr. Jonathan Earls, Miss. Heather Tanner, Dr. Lingyun Zhou, Miss. Yarina Masniuk, and Mr. Huantong Yao for many enjoyable months spent working side by side and discussing our respective experiments. I wish them well in all of their future endeavors throughout their continued careers.

Further thanks go out to my close friends Stephen Twyman and Charles Davidson. Their ever-present advice and influence have been a grounding force for me.

I owe a massive debt of gratitude to my father and mother, Mr. Oyvind and Inger Marie Haukas, who have raised me to be the person I am today and continue to influence my growth in life, even from afar. A huge thanks to my in-laws Mr. Dan and Debbie Dorman for their ever present support. Also a special thank you goes out to my sister, Elise, and my wonderful family of brother and sister in-laws. Finally, I'd like to express my utmost thanks to my dear wife Sally. Her consistency and unfailing love and support have given me the strength to pursue my dreams and ambitions. I will forever be thankful of her encouragement and sacrifices over the years.

DEDICATION

I dedicate this thesis foremost to my Lord and Savior, Jesus Christ,
to my lovely wife Sally Ann Haukas, without whom none of this could have happened,
and to my parents Oyvind and Inger Marie Haukas, who have sacrificed greatly for me
and my family.

CONTENTS

1. INTRODUCTION	1
2. FUNDAMENTALS OF ELECTROSPINNING	5
3. CONFIGURATION OF AN ELECTROSPINNING DEVICE	7
4. FABRICATION OF ELECTROSPUN NANOFIBER SCAFFOLDS	12
4.1. SELECTION OF MATERIALS.....	12
4.2. ELECTROSPINNING PROCESS.....	17
4.3. OPTIMIZING THE PLASMA TREATMENT.....	22
5. CHARACTERIZATION OF ELECTROSPUN SCAFFOLDS	25
5.1. MECHANICAL TESTING.....	25
5.2. SEM.....	28
5.3. WATER CONTACT ANGLE TESTING.....	31
6. CELL GROWTH ON ELECTROSPUN SCAFFOLDS	33
7. FUTURE WORKS	38
REFERENCES	40
APPENDIX	45
VITAE	52

1. INTRODUCTION

Tissue engineering and stem cell research show great promise for treating many diseases. It has the unique potential to bridge the gap between the numerous patients requiring donors and the relatively few donor tissues available. It can also potentially expand lifespan and improve life quality by replacing damaged or diseased organs and tissues using lab-produced alternatives. Although remarkable advancements in tissue engineering have been made in the last two decades, the creation of biologically functional tissues and organs has still been a big technical challenge. One of these challenges is the design and fabrication of an *in vitro* cell growth system that mimics an *in vivo* environment that allows cell-cell and cell-extracellular matrix (ECM) interaction. The primary goal of this study is to develop an electrospun nanofiber scaffold and test it for its capability of supporting cell growth. The long-term goal is to employ this electrospun nanofiber scaffold for directing stem cell lineage-specific differentiation from which biologically functional tissues and organs can be generated and used for clinical applications.

To fabricate these scaffolds, we chose a biodegradable polymer for its high biocompatibility. Synthetic biodegradable polymers are becoming increasingly important materials for tissue engineering. Polymers like poly(ϵ -caprolactone) (PCL), poly(lactide-*co*-glycolide) (PLGA), and poly(ethylene-oxide) (PEO) are emerging as leading biomaterials for construction of tissue engineered scaffolds for promoting cell growth *in vivo* and *in vitro*. An ideal polymer scaffold facilitates cell growth by replicating the many functions of ECM[1] and giving the cells a growth structure and surface on which to interact with each other.

Following several attempts of electrospinning collagen, PCL, and PEO, we chose to use PCL to test this feasibility. The surface of raw electrospun PCL nanofibers is considerably hydrophobic and unsuitable for cell attachment and culture, which requires hydrophilic surface properties in a substrate. To change the PCL nanofiber surface from hydrophobic to hydrophilic, we adopted an oxygen plasma treatment process following electrospinning. We then determined the effect of plasma treatment on hydrophilicity and the mechanical properties of the scaffold. Finally, we tested the feasibility of using these plasma treated electrospun scaffolds for three-dimensional (3D) cell cultures.

Electrospinning is essentially a stable cone-jet manifestation of electro spraying (electrostatic spraying). Electro spraying is a process that can be traced back to William Gilbert, a physician, physicist, and natural philosopher of the late 1500's who is considered to be a pioneer researcher in magnetism. In his publication, he described a phenomenon by which a droplet of water, in the presence of a charged piece of amber, would deform into a cone[2]. Though no further specific observations were made or reported by Gilbert, this is considered to be the first recorded instance of electro spraying. The first quantified experimental work on electrospinning was done by John Zeleny in 1914 when he published his work on fluid droplet activity at the end of metal capillaries[3], presenting experimental evidence for a variety of electro spraying methods, including the cone-jet phenomenon (electrospinning). In 1934 a new electrospinning technique was patented by Anton Formhals for the production of textile yarns[4], and in 1939 a factory was established in the USSR based on Rozenblum and Petryanov-Sokolov's work for producing smoke filters for gas masks. Significant works on the physics and mathematics of the cone-jet formation were later carried out by Sir Geoffrey Ingram Taylor from 1964 to 1969[5], and

subsequently the phenomenon is described today as a Taylor cone. The application of electrospinning as a manufacturing tool in the medical industry and its use in tissue engineering was suggested in by Doshi and Reneker in 1995[6] and has led to massive growth of the field in subsequent years[7].

Initial work surrounding the use of electrospun materials towards cell growth was published by Huang's group in 2001 using a collagen-PEO (poly-ethylene oxide) composite solution[8], followed closely by Matthews' group in 2002 working with collagen and exhibiting cell proliferation on the scaffold[9]. Since then numerous researchers have worked on expanding the application of electrospinning within tissue engineering, including the use of various other polymer blends, ECM components, crosslinking materials, and scaffold treatment methods[10–16].

In seeking out which material is most suitable for fabricating a 3D scaffold for cell growth we examined many recent works related to electrospinning. We found that PCL is an interesting biomaterial and has many desirable traits for supporting cell growth. It has been widely used in tissue engineering and regenerative medicine[17–22]. Powell's group has recently produced an engineered human skin material by utilizing an electrospun collagen-PCL blend scaffolding to serve as a host for keratinocytes and fibroblasts[17]. Lowery's group at MIT recently conducted a series of experiments to further characterize the specific effects of electrospinning parameters on the fiber properties of PCL scaffolds. In doing so they also employed a highly repeatable testing method for seeding consistent and uniform cell populations into their scaffolds using a perfusion seeding system[23].

A general characterization of plasma treated PCL has been previously indicated[24–27], but most experiments reference long treatment time ranges and varying types of plasma (oxygen and argon). Our aim was to analyze favorable results from that data in order to further investigate and optimize operating time and conditions of plasma treatment in order to facilitate scaffolds that support cell growth and proliferation while minimizing degenerative effects on the mechanical properties of the scaffolds.

2. FUNDAMENTALS OF ELECTROSPINNING

Electrospinning is fundamentally based on charge distribution and rearrangement within a polymer solution as it flows through a capillary and across a gap containing a strong electrical field. As a droplet begins to form at the apex of the capillary, its shape and surface tension is initially governed by the viscosity of the polymer solution. With the application of a high voltage near the apex, a flow of positive charge is induced onto the surface molecules of the droplet. As the buildup of these positively charged molecules increases in the droplet the repulsive forces of these mutually charged ions overcome the surface tension, and the resulting conical deformation is known as a Taylor cone[6,28–30]. The Taylor cone ejects a thin strand of the solution from its tip towards the grounded collector plate, and as the strand travels through the air its cross sectional diameter decreases as the solvent is allowed to evaporate. At a point approximately halfway between the charged capillary and the collector plate, the continually thinning strand begins to exhibit a whipping motion which is barely visible to the naked eye. This whipping motion is governed by the strength of the electric field, and travels in a completely random pattern onto the center of the collector plate. As the strength of the electrical field increases, the diameter of this collection area is decreased as the whipping strand undergoes a stronger attraction to the collector. The observable diameter of the resulting deposited scaffold does indeed remain consistent when identical electrospinning parameters are maintained, allowing for a repeatable process with which to generate multiple samples for testing. It should be pointed out that the strand remains whole and does not break up or separate at any point in this process. The resulting scaffold should not exhibit and evidence of incomplete strands or terminal end points. Any indication of beginning and ending of the strand under scanning

electron microscopy (SEM) observation likely indicate errors in the electrospinning process and inability to maintain a constant stream from the needle and syringe.

3. CONFIGURATION OF AN ELECTROSPINNING DEVICE

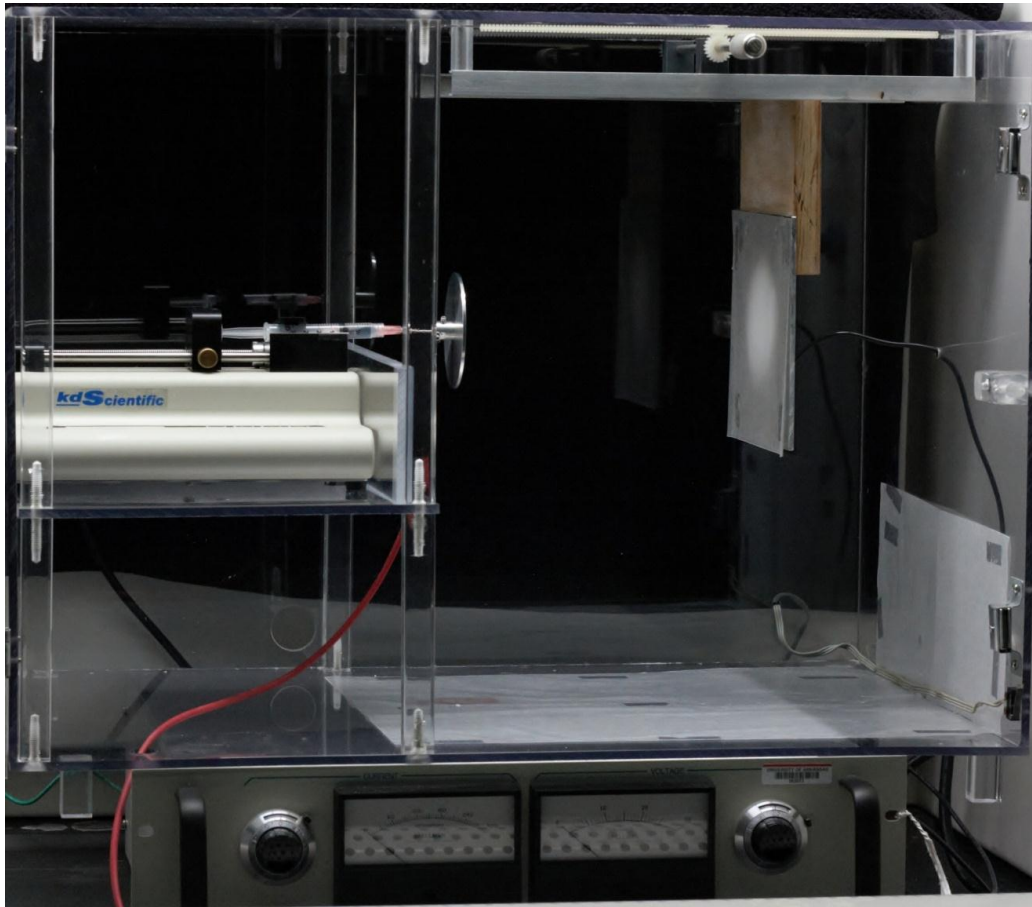


Fig. 3.1. Electrospinning apparatus setup. The setup consists of a Spellman CZE 1000R high-voltage power supply located beneath the unit, a KD Scientific KDS-101 syringe pump with mounted syringe and needle, and a charge distribution plate, high voltage wire (red), and grounded collector plate (black). The enclosure was custom made from polycarbonate sheeting and has a door fitted with a safety switch to disable the high voltage when the door is opened.

We assembled our own electrospinning apparatus based on the established electrospinning principles and other published descriptions of electrospinning arrangement. Our assembly included a custom-built polycarbonate enclosure fitted with a shelf for the syringe pump and a grounded target which can be adjusted to change the distance from the syringe pump. We opted for a horizontal system based on observing a similar setup in other labs. The collector distances can vary from 10 to 30 cm. Based on the literatures published at the time of construction and

assembly this range was deemed sufficient for our purpose, as the majority of our electrospinning occurred at a distance of 15-20 cm. The selected power supply is a Spellman CZE 1000R with a maximum voltage of 30 kV (reversible) and maximum power of 9 watts. It was used with a 3 foot shielded wire connecting the power output to a collar-plate assembly. We designed a unique aluminum collared plate in order to establish a consistent and uniform electric field for our experiments and prevent the electrospinning stream from deviating from the center of the collector, hampering our ability to reproduce consistent nanofiber meshes. The plate was milled from a 3" diameter aluminum cylinder. It is 1/8" thick with one face completely flat and the other containing a cylindrical protrusion measuring 1/2" in diameter and 1/2" tall. Through the center of this plate and collar is a 0.06" hole through which an 18G needle can be placed. Attached to the collar are a set-screw for securing the plate to the needle itself, and a separate screw and washer for attaching and clamping the exposed end of the power supply wire to the assembly in order to establish and maintain consistent contact and current. The plate allows for the positive current to be symmetrically applied to the needle and solution, and reduces any variance in sample thickness and arrangement of fibers during electrospinning. Over the course of our experiments we experienced a frustrating obstacle in producing uniform samples. At times we could not see the Taylor cone itself but only the thin strand which it produced, ejecting from along the circumference of the needle tip while slowly cycling in repeated circles. Over time we were able to rectify this issue by shifting the charge plate closer to the tip of the needle. As shown in **Fig. 3.2** the application point of the charge determines whether or not the solution is able to maintain its surface tension through to the tip of the needle and form a Taylor cone.

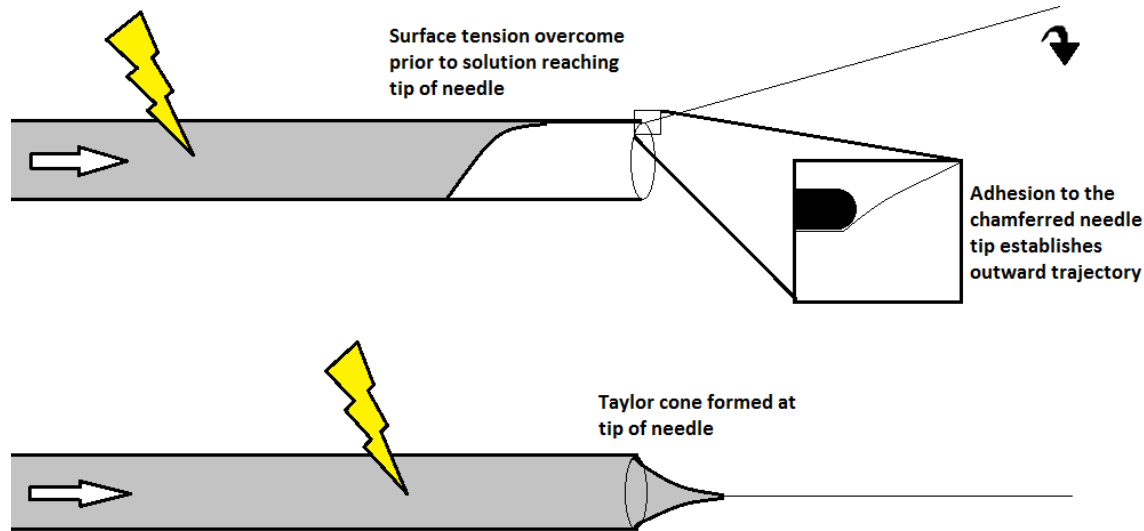


Fig. 3.2. Effect of distance between voltage application and needle tip. The distance between the voltage application point and the needle tip is important in obtaining a proper Taylor cone. As evidenced in this drawing, if the tip is too far away from the voltage application point, the repulsion of like-charge particles will cause the solution to form a thin stream within the needle and lead to issues with sample collection.

We conducted all of our final experiments with a distance of 4 mm from needle tip to the leading wall of the charge distribution plate. Further examining this setup we noted that the charge is first introduced approximately 2.94 cm from the needle tip for our successful experiments.

The collector plate is a 6" square aluminum plate, 1/8" thick with a threaded screw for attaching the ground wire to the rear of the plate. The plate is mounted to a wood block for insulating purposes, which is subsequently mounted to a rail assembly fitted into a gear-and-rack system on rails for flexibility, precision, and repeatability when manipulating the distance from needle to collector. The syringe pump is a KD Scientific KDS-101, capable of holding syringes ranging in size from 10 μL to 60 ml, giving it flow rate options ranging from 0.1 $\mu\text{L/h}$ to 506 mL/h. Of note we also decided to make a custom polycarbonate divider and support for the syringe pump, allowing the entire assembly to be used as a vertical system by standing it on its right-hand wall, and also providing electrical shielding for the charged wire, plate, and needle. We observed

several instances of the charge plate and wire shorting to the grounded body of the syringe pump, severely disrupting the electrospinning stream and leading to spraying of individual droplets and lack of uniformity in the electrospun sheets produced.

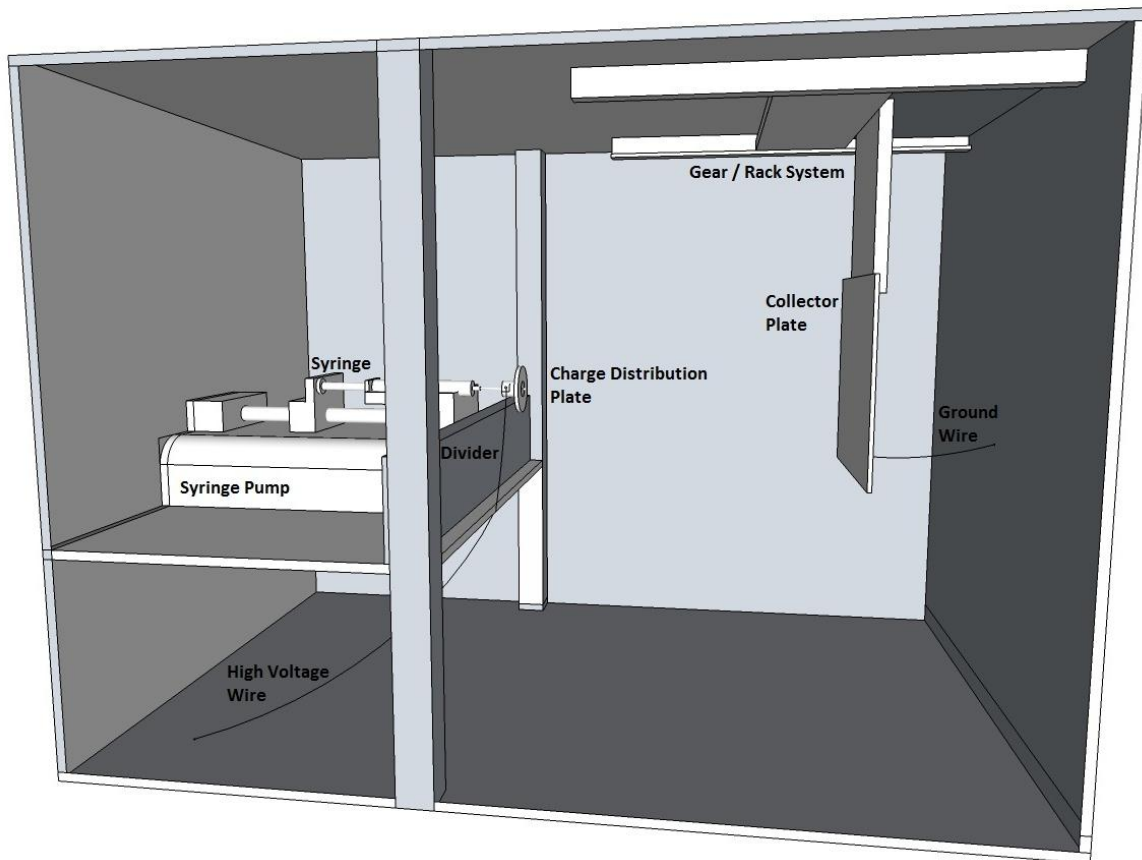


Fig. 3.3. 3D Model of the electrospinning assembly. The assembly is a custom-built polycarbonate enclosure fitted with ports for wiring and a safety cut-off switch built into the door. The divider portion gives us the option of running the entire system vertically, and also provides insulation between the charged plate and the grounded shell of the pump.

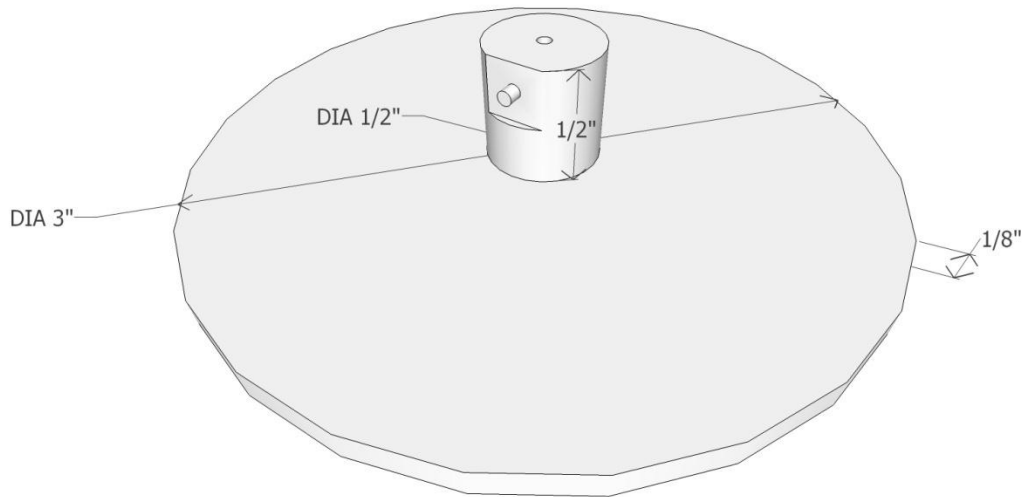


Fig. 3.3b. Diagram and dimensions of the aluminum charge distribution plate. The downward face is completely flat and smooth, producing a uniform positive electrical field. The central hole for the needle is large enough to accommodate an 18G needle, and contains a set-screw which can be tightened onto the needle to provide consistent contact and allow for higher gauge needles to be used with this assembly.

The entire electrospinning assembly is setup within a chemical fume hood in order to avoid any harmful effects of the evaporating chloroform and methanol mixture.

4. FABRICATION OF ELECTROSPUN NANOFIBER SCAFFOLDS

4.1. Selection of Materials

Our initial choice of material for fabricating electrospun nanofiber scaffolds was an ECM component. After examining a considerable amount of research on electrospinning ECM proteins[9,31–35] we decided to begin our work with rat tail collagen-I.

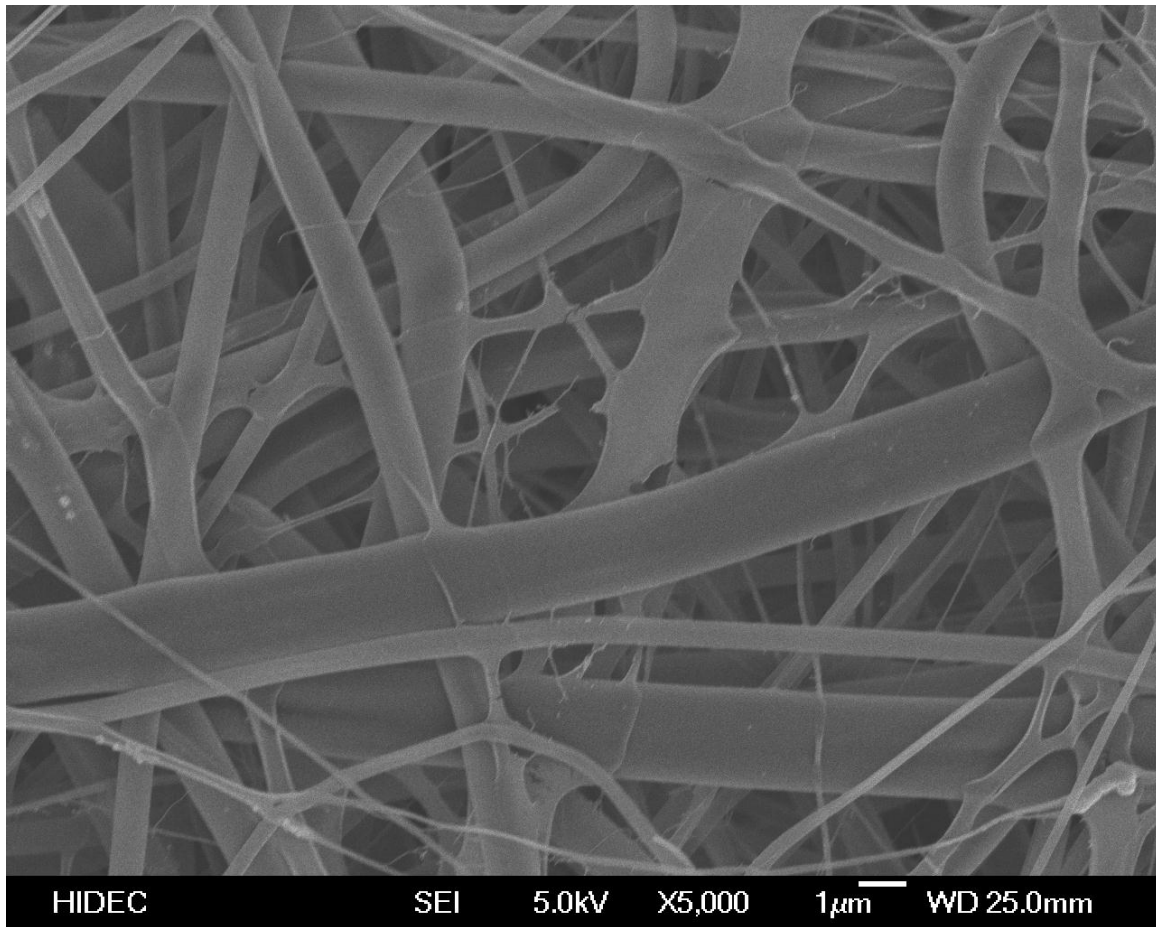


Fig. 4.1. SEM image of electrospun collagen-I fibers. Here we see that the fiber and pore sizes are inconsistent in size, and the fiber shape is not maintained throughout the sample. Many fibers are not purely cylindrical, and branching fibers indicate that the electrospinning process was not successful in producing a singular uniform strand throughout the sample

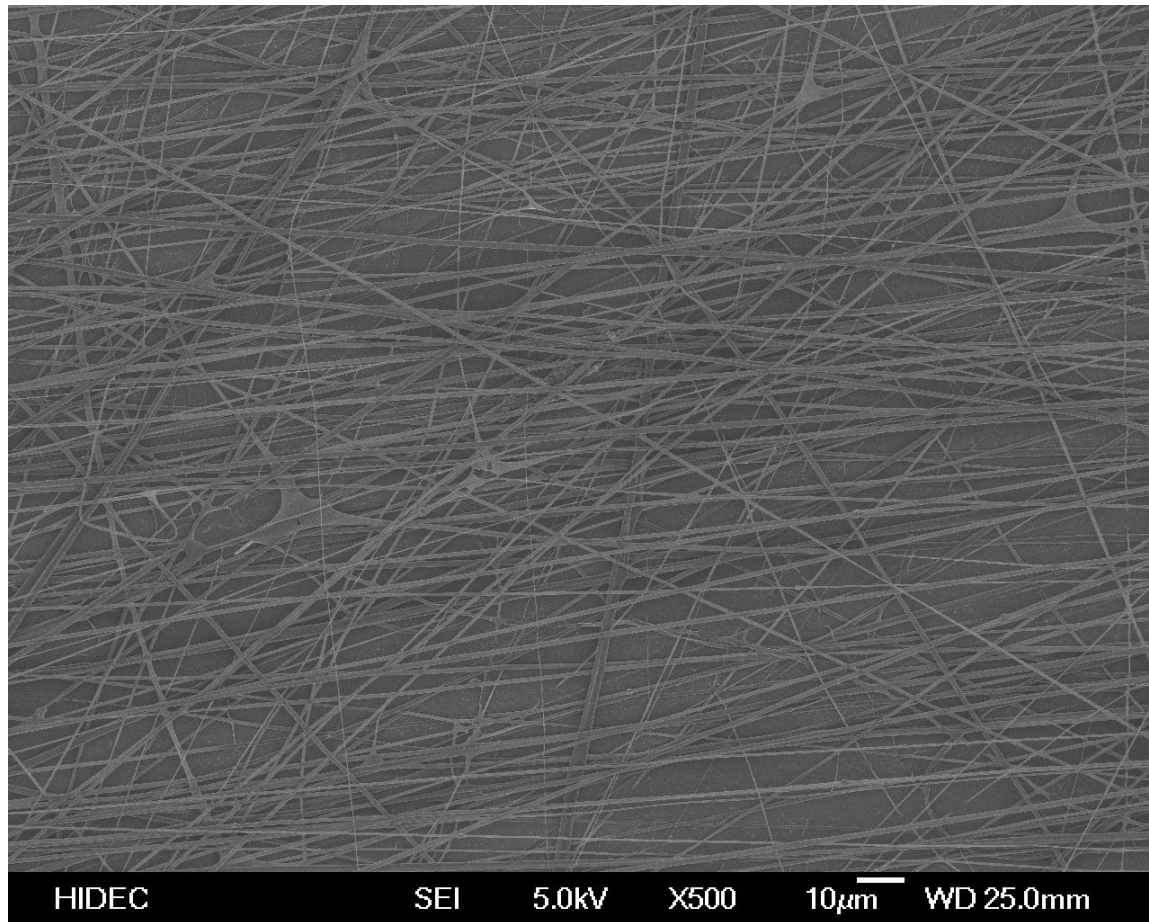


Fig. 4.2. SEM image of electrospun collagen-I fibers collected onto a charged polystyrene slide. This sample was produced under similar conditions to Figure 4.1, but the charged nature of the surface clearly affected the distribution and orientation of the fibers during deposition. A clear “X” pattern can be seen in addition to a large number of fibers oriented horizontally. Again we see the branching fibers and some variation in fiber size, though not as much as the non-slide sample.

Our plan at that time was to examine different ratios of collagen-I blended with fibronectin and laminin, either in our electrospinning solution or as a secondary treatment coating. Through multiple different collagen concentrations and solvent mixtures we were unable to produce a homogenous and consistent scaffold. Fiber shape and structure was anomalous as seen in **Fig. 4.1** and indicated that there were inconsistencies between samples produced with the same parameters. In our search for a collector covering to allow for simple retrieval of our samples we also experimented with polystyrene slides mounted with double-sided tape. The result, as seen

in **Fig. 4.2**, was a particularly linear arrangement of the deposited fibers, displaying the effect of the charged nature of the slides themselves, and even contributing to an increased observable consistency of the collagen fibers. Unfortunately we still observed the branching of fibers at various points indicating a lack of continuity in the strand during the deposition process. Also – a rigorous collection of fibers at right angles to each other would not seem to provide the same environment we can achieve with a random arrangement.

In addition to these observations, we had problems identifying a suitable crosslinker for our collagen scaffolds. Crosslinking is required for bounding the collagen fibers together in order to prevent the scaffold from degrading when submerged in a cell culture medium. Glutaraldehyde (vapor) is often used for collagen crosslinking [12,13,36] and has been adapted in similar experiments for that purpose, but we were wary of its cytotoxicity[37–40] and decided to test other crosslinkers. Our search led us to try proanthocyanidin, a naturally occurring grape seed extract which has been previously shown successful for crosslinking[38,40]. We attempted to use proanthocyanidin for both collagen and chitosan samples, but were unsuccessful in obtaining suitable samples for SEM analysis and cell growth following attempts at lyophilization and other dehydration methodologies.

We briefly experimented with the use of PEG (polyethylene glycol) but also struggled to establish a suitable electrospinning procedure to produce results with the desired material properties. We were, however, able to leverage much of the information learned during the PEG electrospinning attempts when shifting towards our third material selection. Much of the work done in attempts to optimize the electrospinning setup itself and to create a uniform electrical

field was accomplished during the PEG electrospinning experiments. The droplets shown in **Fig. 4.3** indicate an inconsistent flow of material during electrospinning and an inability to overcome the surface tension of the solution with the parameters applied. Flow rates which are too high for the applied voltage lead to droplet formation at the tip of the needle, which is eventually deposited onto the sample as the charge grows large enough to propel the entire droplet into the collector. An increase in voltage does not always provide a balance to the flow vs charge equilibrium, though a proper balance is indeed necessary for a homogenous electrospun material.

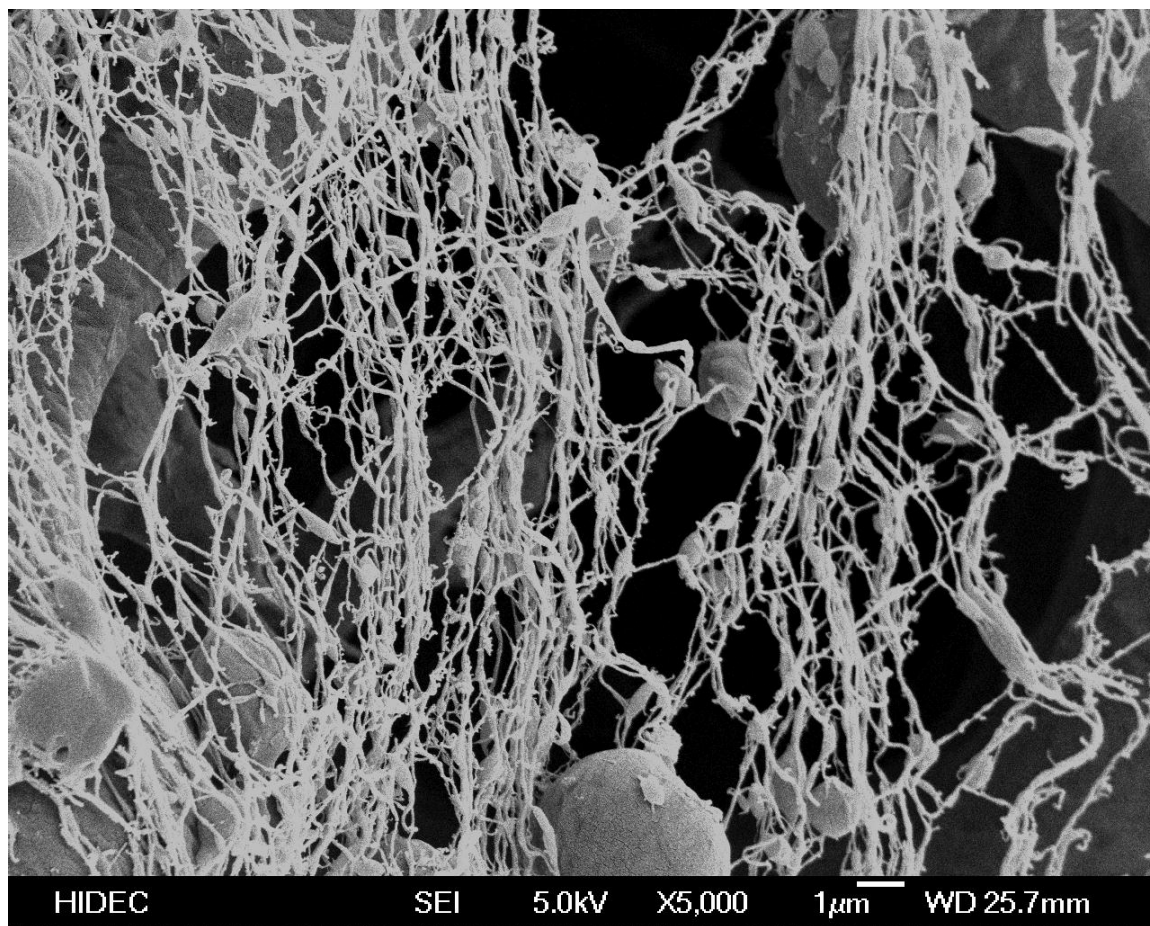


Fig. 4.3. Electrospinning of PEG. From these images we can see the non-uniform nature of the scaffold and the presence of randomly sized globules disrupting the mesh structure

We chose to shift our focus to electrospinning PCL, and based on previous work[23] we made some decisions concerning the characteristics that we were looking for in our final material (pore

size, fiber size, arrangement). We conducted several experiments with varying PCL concentrations, solvents, and electrospinning parameters to determine the ideal parameters for our specific electrospinning setup and confirm our ability to produce uniform and reproducible scaffolds with our desired characteristics (Figs .4.4 and 4.5).

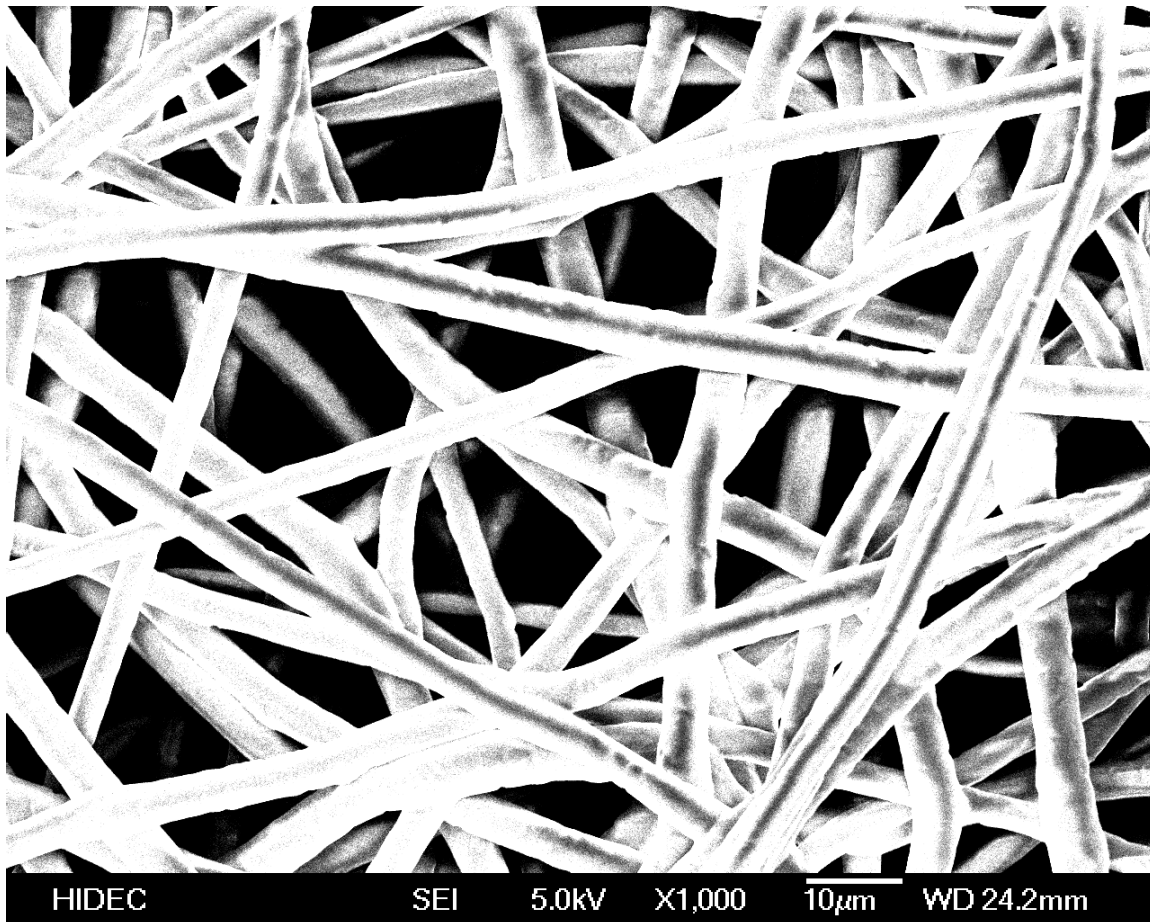


Fig. 4.4. Untreated Electrospun 15% PCL @1000x. The 15% PCL exhibited a thicker average fiber diameter, but showed positive signs in terms of pore consistency, fiber consistency, and uniform arrangement and distribution.

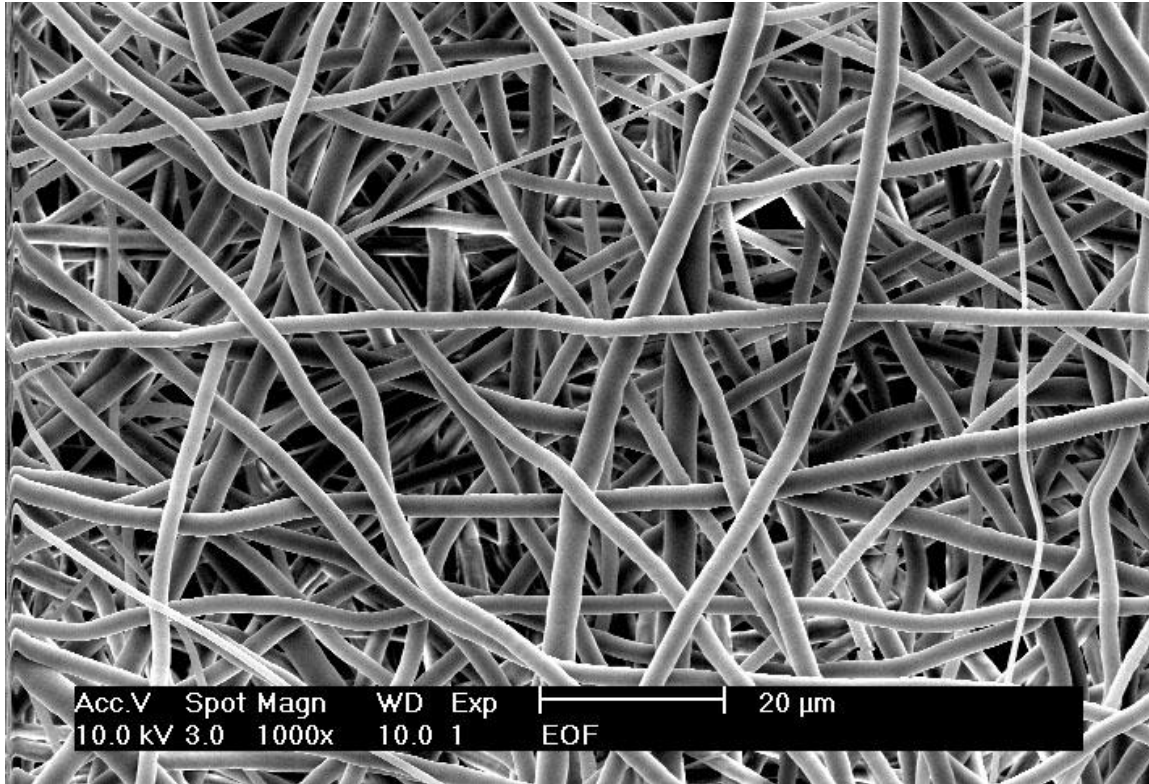


Fig. 4.5. Untreated Electrospun 11% PCL @1000x. The 11% PCL samples produced consistent size and fiber morphology with a smaller observable fiber diameter than the 15% attempts. Based on these characteristics we chose to use this as our experimental template.

The 15% PCL exhibited a relatively thick average fiber diameter, but showed positive signs in terms of pore consistency, fiber consistency, and uniform arrangement and distribution. The 11% PCL samples produced consistent size and fiber morphology with a smaller observable fiber diameter than the 15% attempts. Based on these experiments we decided on 11% PCL (~80,000 mw) in a solution of chloroform and methanol with a 3:1 ratio (respectively).

4.2. Electrospinning Process

Initial preparation for electrospinning included dissolving the solute in the selected solvent, allowing time for the solution to mix and become homogenous. For our experiments we used

11% PCL in chloroform:methanol (3:1). Under a chemical fume hood we mixed 22.5 ml of chloroform with 7.5 ml of methanol and quickly added 3.3 g PCL (~80,000 MW – Sigma). The mixture was placed in a shaker overnight at 250 rpm at 30°C.

The syringes we used were standard BD polypropylene Luer-Lok 3-ml syringes, with an inner diameter of 8.59 mm. We used 14G needles to slowly draw 1.2 ml of a polymer solution into the syringe, as the solution's high viscosity made it particularly difficult to draw with any smaller needles without introducing many bubbles into the syringe. The syringe was set on its end (tip up) for 5-10 min to allow bubbles to work their way out of the syringe. The needles used for electrospinning are Howard Electronics JG18-1.5P 18G, 1.5" long, ID=0.038" and OD=0.049", and were swapped onto the syringe once the bubbles had been removed. Plain wax paper was mounted on the face of the collector plate with double sided tape, making sure not to bend or crinkle the paper in the mounting process as this would lead to noticeable abnormalities in the final scaffold. Wax paper allows for an ideal sample removal process as it does not require any amount of force to separate the scaffold sample from the paper. The power supply was set to its max at 30 kV and the distance from the mounted syringe/needle tip to the collector plate was set to 20 cm. The syringe and needle were mounted into a horizontal syringe pump and the charge distribution plate was secured onto the needle with its face 4 mm away from the tip of the needle. The needle was initially primed with a controlled amount of solution using a syringe pump. The power supply was fitted with a kill-switch incorporated into the door mechanism of the electrospinning assembly, allowing to have the power supply switched on and use the door to act as an on/off mechanism. The syringe pump was set to a rate of 95 $\mu\text{L} / \text{min}$, having been calibrated to match the inner diameter of the syringe (8.59 mm). With the door open and power

on, the syringe pump was turned on and as soon as any solution was visible at the tip of the needle the door was closed, immediately activating the full 30 kV of the power supply.

Electrospinning was monitored from outside of the fume hood to confirm a consistent stream and no instances of electrospaying, which would have rendered that particular sample useless for our experiment.

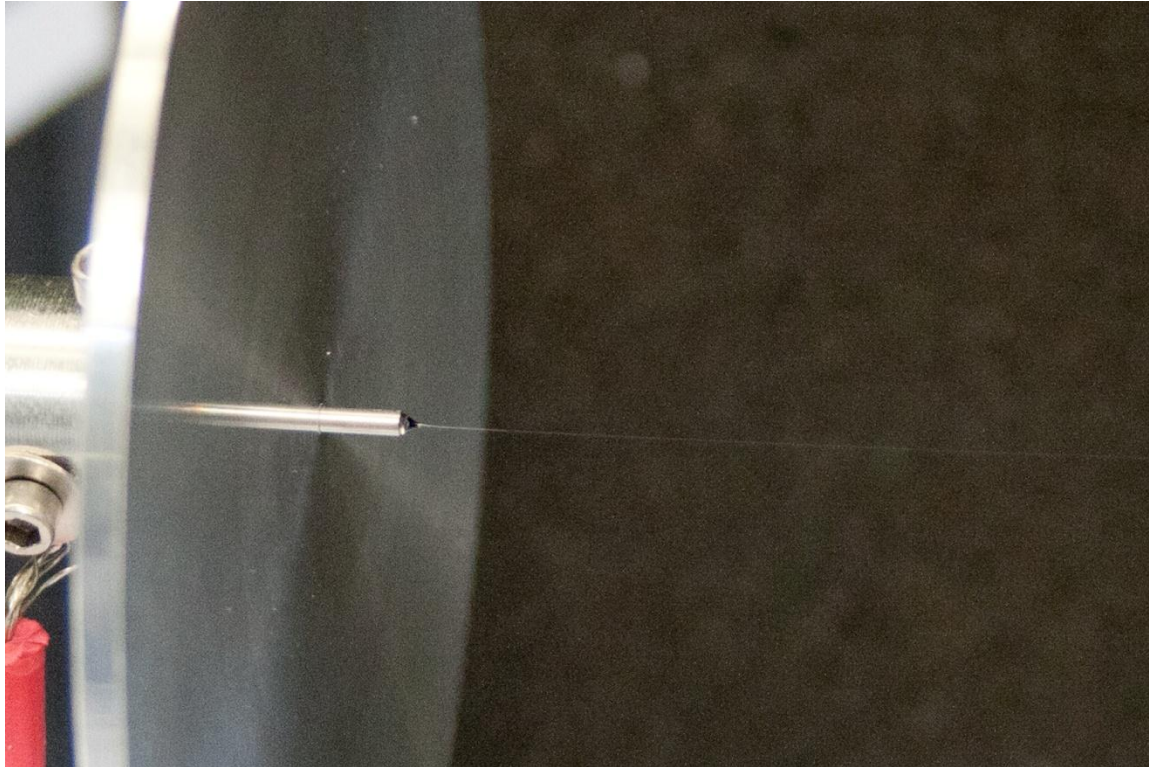


Fig. 4.6. View of the Taylor cone formed at the tip of the charged needle. Here we see the charge distribution plate and electrospinning process, with the Taylor cone clearly visible at the tip of the needle. Also note the slightly visible set screw securing the plate to the needle (from above), and the secondary screw and washer ensuring a tight and consistent electrical contact area for the high voltage wire from the power supply.

Fig.4.6 captures the Taylor cone and its ejected stream, displaying the shape and stability obtained with proper electrospinning parameters. A straight, consistent stream was observed travelling approximately 50% of the distance towards the collector (~10 cm) at which point it became invisible to eyes. The use of a laser pointer allowed the observation of the very

beginning (5 mm) of the destabilization region and whipping motion, while a camera was able to capture varying amounts of the whipping strand due to the reflections of light on the strands. In **Fig.4.7** we captured the destabilization area as it began to disrupt the strand.



Fig. 4.7. View of needle with fiber destabilization and start of whipping motion

It is noted that the relative locations of destabilization regions to the charge plate and collector plate remain constant during the electrospinning process, as long as the solution flow rate is sufficient and both rate and voltage remain constant. **Fig. 4.8** contains a closer view of the rapid increase in circumference following the initial whipping motion from the point of instability of the strand. Observing this image, there does not seem to be a consistent pattern or path followed by the whipping strand. This is likely due to the continued repulsion of the strand from itself, as it is highly charged with positive ions. The continued repulsion of the unstable region would indeed continually disrupt the whipping pattern and manner of deposition.

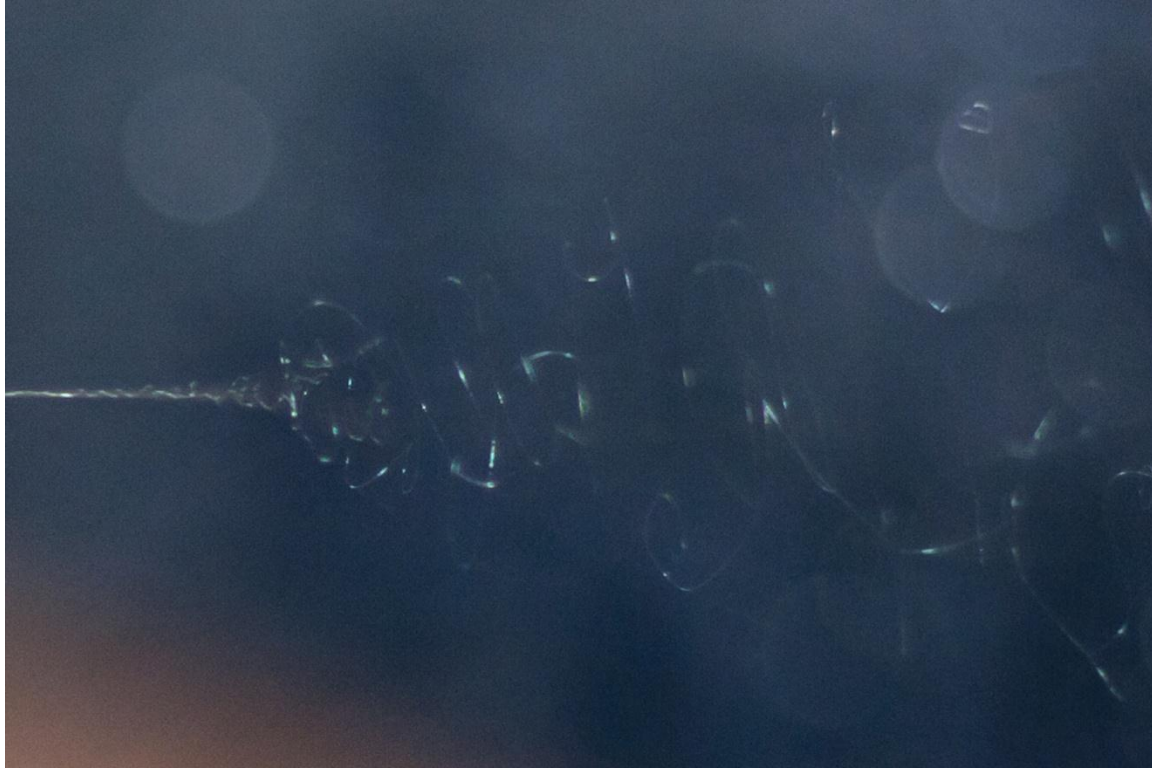


Fig. 4.8. Close-up view of strand with whipping motion.

Analysis of this image indicates that the strand is one continuous strand which is subject to a whipping motion in a steadily increasing radius. Voltage and collector plate distance play a role in the diameter of the resulting sample, as it governs the distance between destabilization and the collector plate and thus the distance over which expansion of the whipping thread can take place. Once the solution reached 1.2 ml the syringe pump stopped and voltage was immediately turned off by opening the door slightly. The vent hood was turned on to remove and cycle the air from within the chamber. It was always off during the experiment to prevent air flow from disrupting the strand and deposition. The wax paper holding the sample was removed and immediately placed in a sterile environment. Once sufficient samples were generated – the ~4 inch diameter samples were plasma treated before being cut into small pieces for experiments. The tensile

samples were cut using a template (**Fig. 5.1b**) and the meshes used for cell growth were prepared using a 13 mm circular punch to facilitate placement in a cell culture plate.

4.3. Optimizing the Plasma Treatment



Fig. 4.9. Plasma treatment was conducted in the Plasma Therm SLR 720 RIE. Reactive Ion Etching with oxygen was performed at the University of Arkansas HIDEc center to introduce hydrophilic properties to the PCL scaffolds.

One of the major issues that must be addressed before electrospun PCL nanofiber scaffolds can be employed for growing cells is its highly hydrophobic surface. Without any treatment, electrospun PCL nanofibers exhibit a water contact angles of $\sim 130^\circ$ [26] as seen in **Fig. 4.10**.

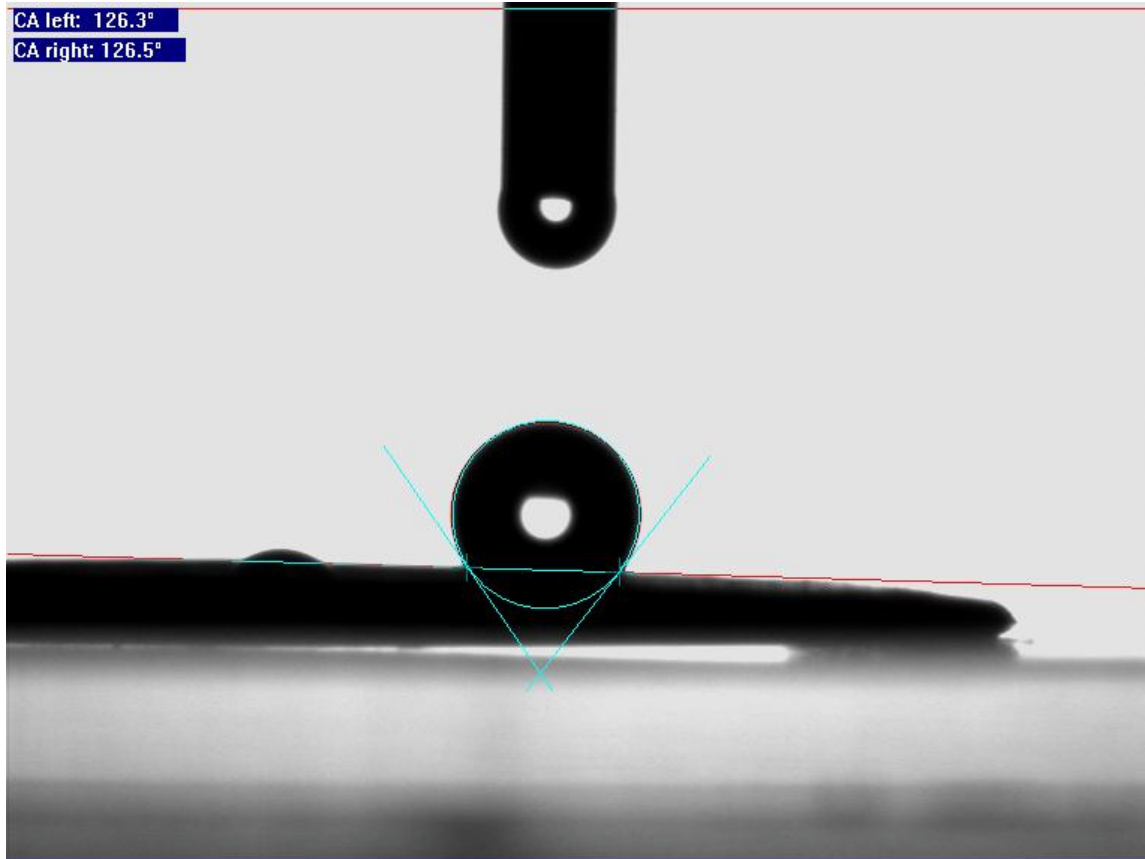


Fig. 4.10. Water contact angles for untreated electrospun 11% PCL

Studies suggested that treating the scaffolds with oxygen plasma for either 5 or 10 min would greatly reduce this angle to below 20° . The water contact angle for this newly hydrophilic surface is difficult to capture with a high speed camera due to the instantaneous absorption of the droplet into the surface of the scaffold. To obtain quantifiable contact angles we used glycerol to test relative hydrophilicity. We adapted this technique from Martins' group, who conducted a specific study which looked to quantify several plasma treatment gases and broad parameters in order to determine which yielded the most favorable biological compatibility[26]. The data set they generated clearly suggests that the use of oxygen plasma at 30 W can achieve the best contact angle, with periods of 5 and 10 min showing similarly significant improvements over the

other treatment parameters. **Fig. 4.11** exhibits the glycerol contact angle results from their experiments.

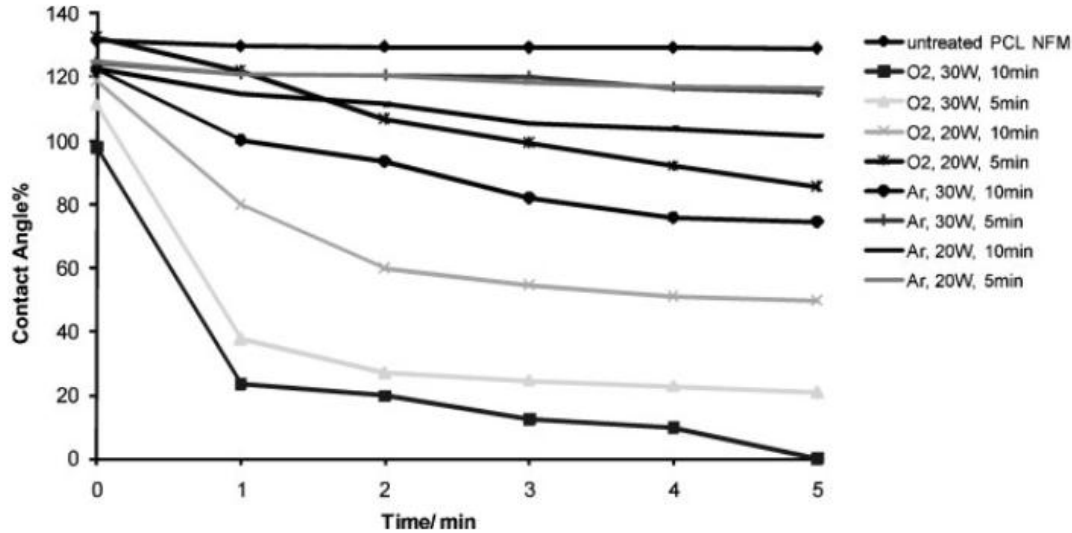


Fig. 4.11. Contact angle of Glycerol with plasma treated electrospun PCL[26]. Contact angles for various plasma treatment methods of PCL over time. This material served as the inspiration to conduct a more granular assay for our experiment. Adapted from Martins, “Surface modification of electrospun polycaprolactone nanofiber meshes by plasma treatment to enhance biological performance.” 2009, Small.

For our experiments we chose to use these effective treatment parameters, but to alter the time of treatment in order to achieve a more specific optimization of the surface modification. This ideal treatment for PCL is oxygen plasma at 30 watts and 13.56 MHz, which we replicated at a pressure of 100 mTorr and flow rate of 20 sccm following the treatment protocols for our specific equipment.

5. CHARACTERIZATION OF ELECTROSPUN SCAFFOLDS

5.1. Mechanical Testing



Fig. 5.1a. Instron 3365 system for determination of elasticity of electrospun scaffolds. Instron setup with clamps in order to test tensile strength and obtain a load curve for the test sample.

To test the mechanical strength of the PCL electrospun scaffolds we used an Instron 3365 Dual Column Tabletop Testing System with a 500 N load cell. The thickness of the scaffolds was determined using a Marathon Electronic Digital Micrometer with an accuracy of 0.002 mm. Samples were treated, with varying exposure times, to oxygen plasma in a Plasma Therm SLR 720 RIE at 30 watts, 13.56 MHz at a pressure of 100 mTorr and flow rate of 20 sccm. Our selected plasma treatment times were 30 s, 90 s, 3 min, and 5 min. Treated samples were cut

into 50 mm x 10 mm strips and paper tabs (10 mm x 10mm) were attached to each end with double-sided tape, leaving a gauge length of 30 mm (**Fig. 5.1b**).

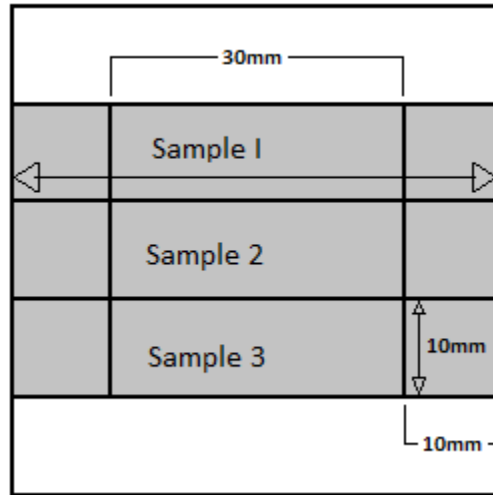


Fig. 5.1b. Tensile sample template instructions. This entire template was cut from paper, and the middle 30x30mm section was cut out completely. The 10x10mm sections were left intact and fitted with double sided tape, and then attached to an entire sample (typical sample diameter was ~100mm) in its complete “hollow square” form with the tape facing down onto the sample. A scalpel was used to carefully cut the samples into 50x10mm strips, leaving a 30mm gauge length and 10mm mounting tabs at each end.

The tabs were mounted into the testing clamps, and samples were put under tensile load with a crosshead speed of 15 mm/min. Readings were taken every 50 ms and two identical samples were tested for each treatment length, including an untreated sample for comparison. The results indicate the average values from these two readings. Our initial thoughts concerning the tensile strength of the scaffolds led us to hypothesize that the plasma treated samples would have a higher tensile strength due to the increased number of bonds created at the intersection points of the fibers. We thus posited that this effect would create an increased friction at each and every intersection of the fibers –increasing both the tensile and shear strength of the material. Our tests suggested a mixed set of results in reference to this hypothesis. Through our testing we found that certain plasma treatment lengths do indeed increase the mechanical strength of the scaffolds.

Curiously, we also noticed that the correlation between treatment time and strength was not linear, with the 90 second treatment producing the weakest samples.

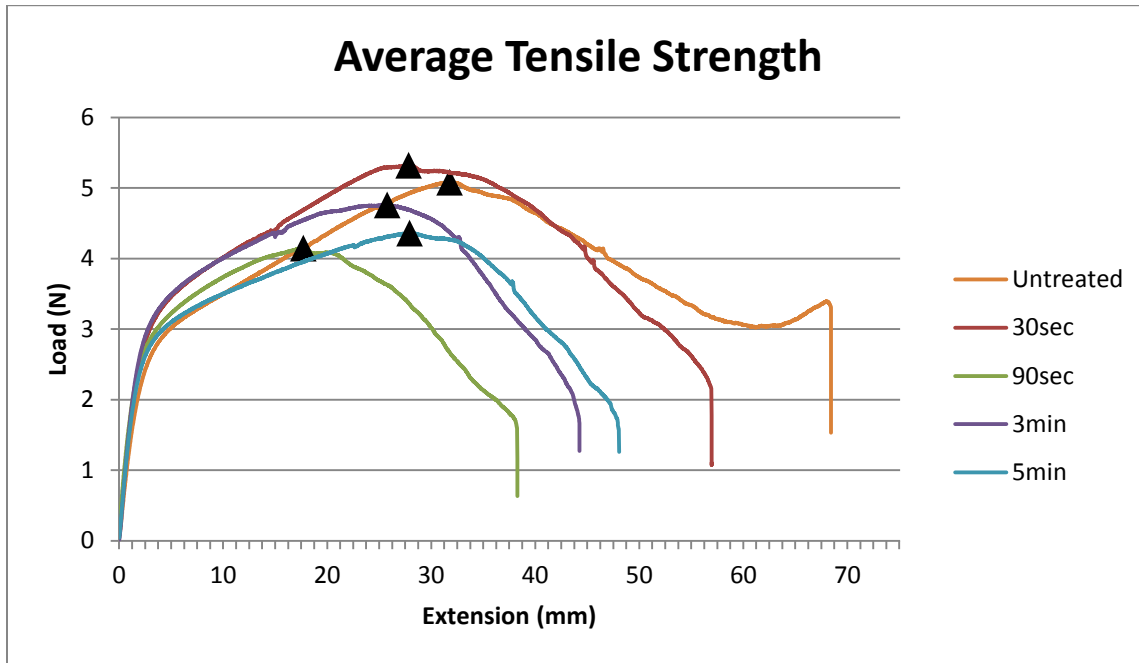


Fig. 5.2a. Tensile strength of electrospun 11% PCL scaffolds with varying oxygen plasma treatment times.

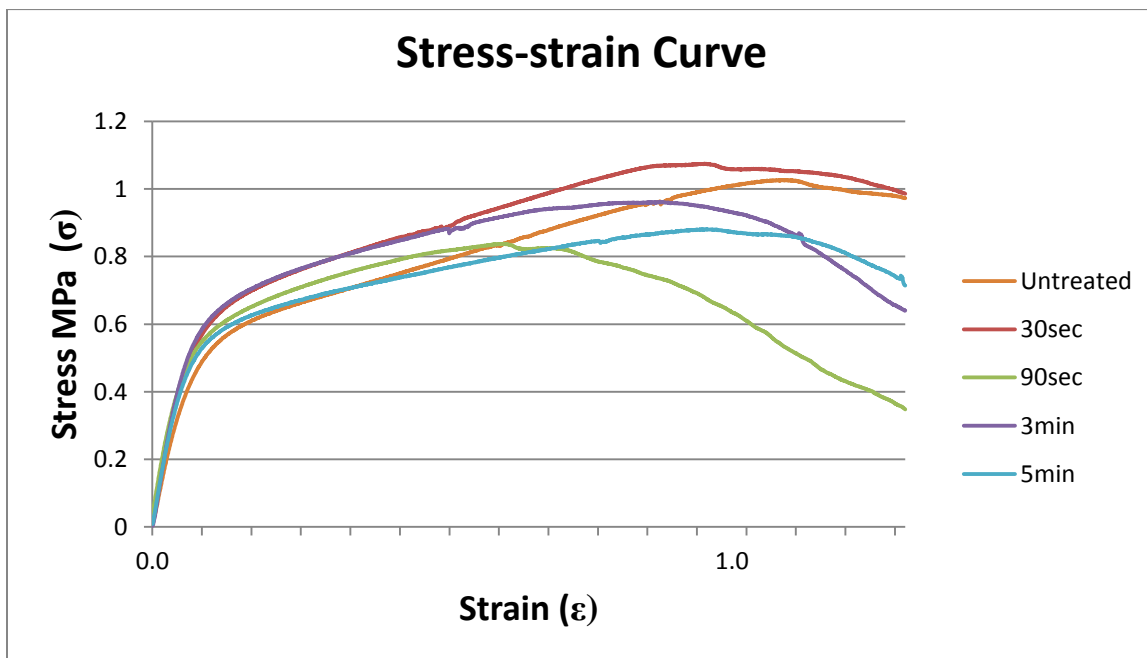


Fig. 5.2b: Stress-strain curve of electrospun 11% PCL scaffolds with varying oxygen plasma treatment times.

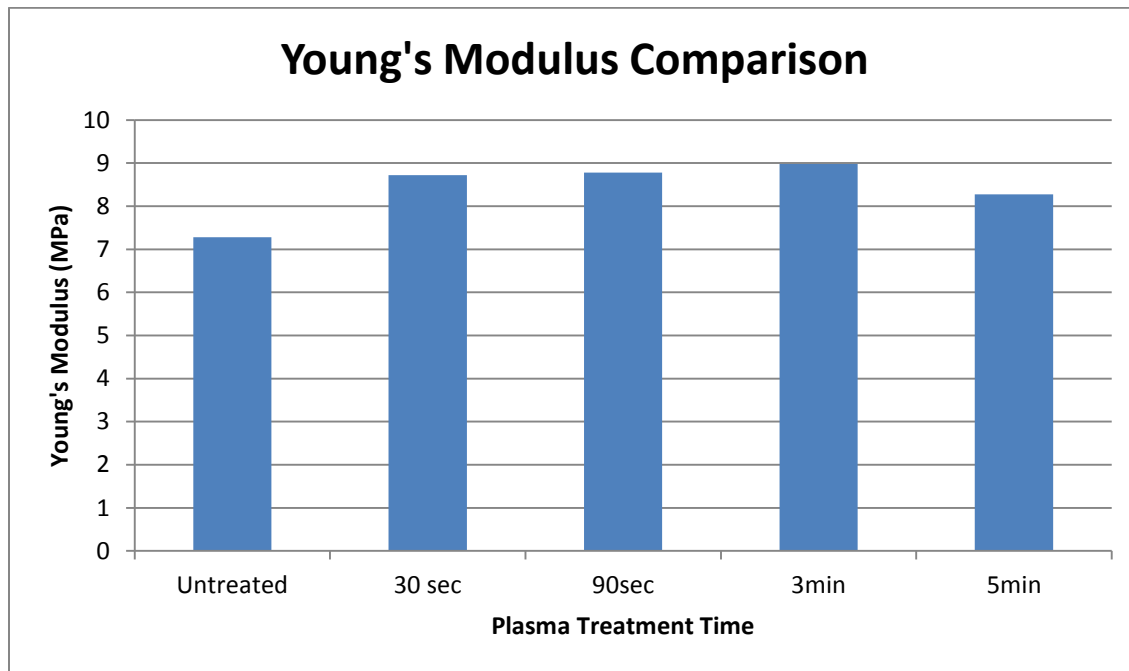


Fig. 5.3. Young's Modulus comparison of electrospun 11% PCL scaffolds with varying oxygen plasma treatment times.

Based on these observations we stipulated that the plasma treatment, which changes the structure of the molecules and their interactions with each other, has the potential to reduce the inherent tensile strength of the individual fibers while simultaneously forming cross-links with other fibers. This leads to an initial observable increase in the overall structure's tensile strength (30s sample) at the cost of incrementally decreasing the individual fiber strength, as evidenced in the remainder of the samples. Accordingly, it endows a membrane with both an induced hydrophilicity and an increased tensile strength when treatment time is limited to 30 seconds.

5.2. SEM

To examine the microstructure of the electrospun PCL scaffolds, the samples were carefully cut and placed on SEM testing bullets with double-sided carbon tape before being gold-coated with

an Anatech Hummer VI-A sputter coater for 150 s at a current of 15 mA and pressure of 18 mTorr. Samples were then observed by SEM in a JEOL JSM-6335F at 5kV. As shown in the following SEM micrographs, the scaffolds display consistent pore sizes, fiber diameter, and fiber distribution, and are indicative of all the samples that were observed and used in our experiments.

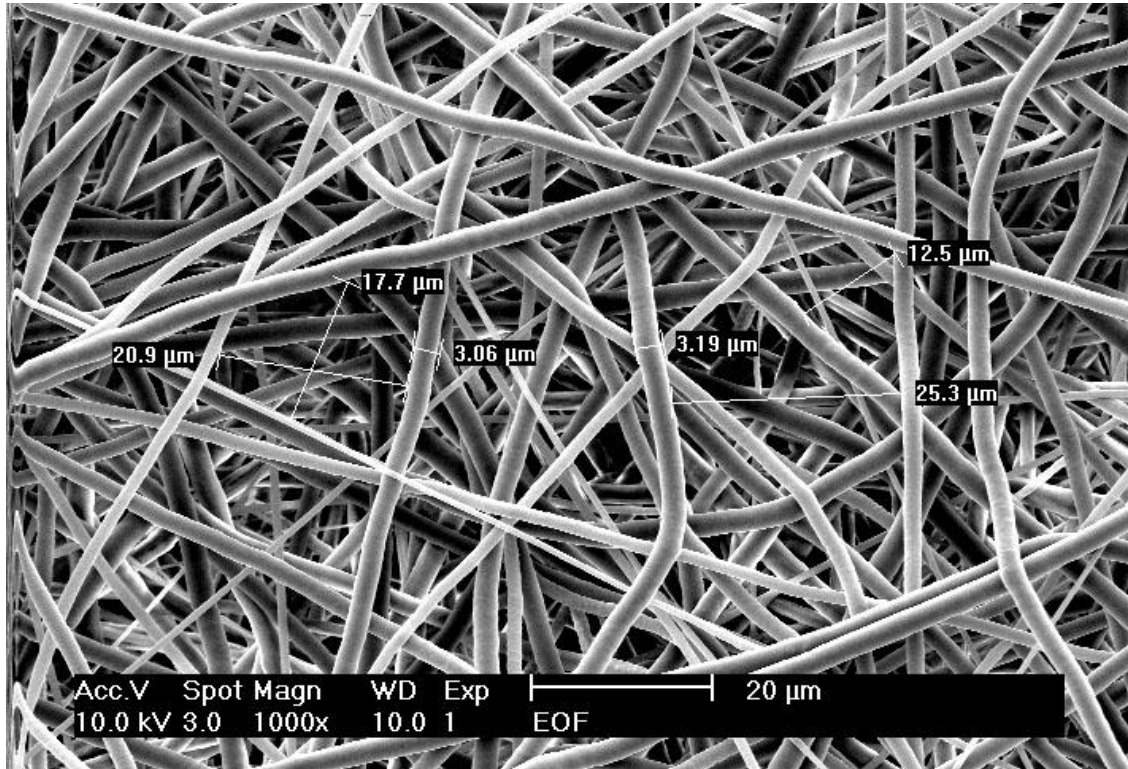


Fig. 5.3. 1000X SEM image of 11% PCL in chloroform:methanol (3:1). Here we can see the fiber distribution and random arrangement throughout the scaffold. No visible evidence of splitting fibers and no gross variation of fiber diameter from the 3μm observable average.

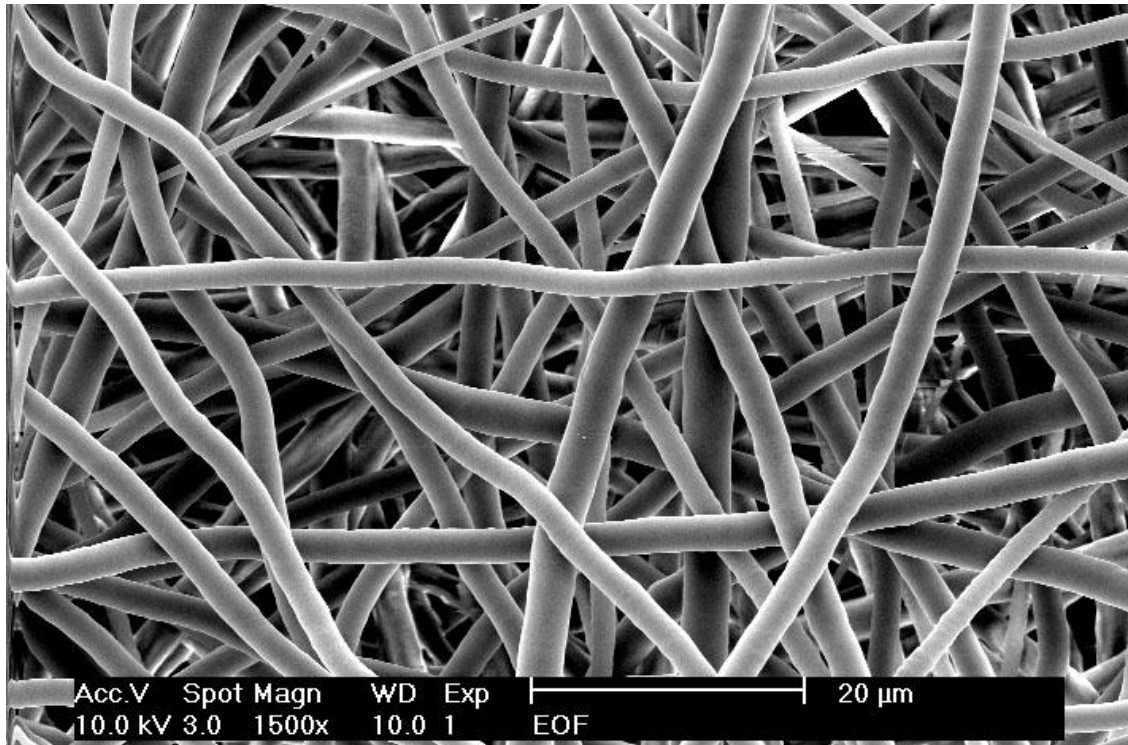


Fig. 5.4. 1500X SEM image of 11% PCL in chloroform:methanol (3:1). A separate sample showing once again the fiber morphology and consistency throughout the sample.

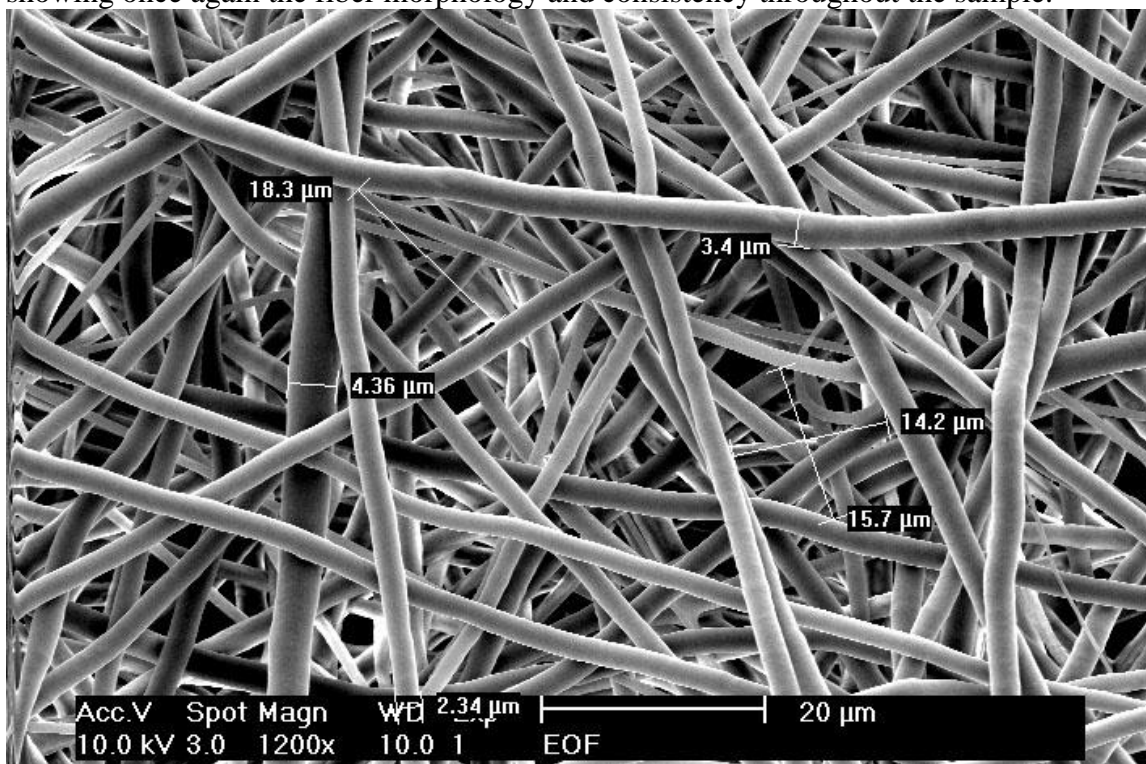


Fig. 5.5. 1200X SEM image of 11% PCL in chloroform:methanol (3:1).

5.3. Water contact angle testing

Initial attempts to determine water contact angle of the plasma-treated scaffolds by utilizing a high speed camera did not capture sufficient data due to a rapid absorption of the water droplets. To overcome this difficulty, we changed our syringe and needle to accommodate glycerol's increased viscosity, which allowed us to capture consistent data and to compare and quantify the hydrophilic effects of different plasma treatment times. Through a high speed camera setup we captured data over a period of time and plotted the contact angles and rate of uptake by the scaffold material (Fig.5.6).

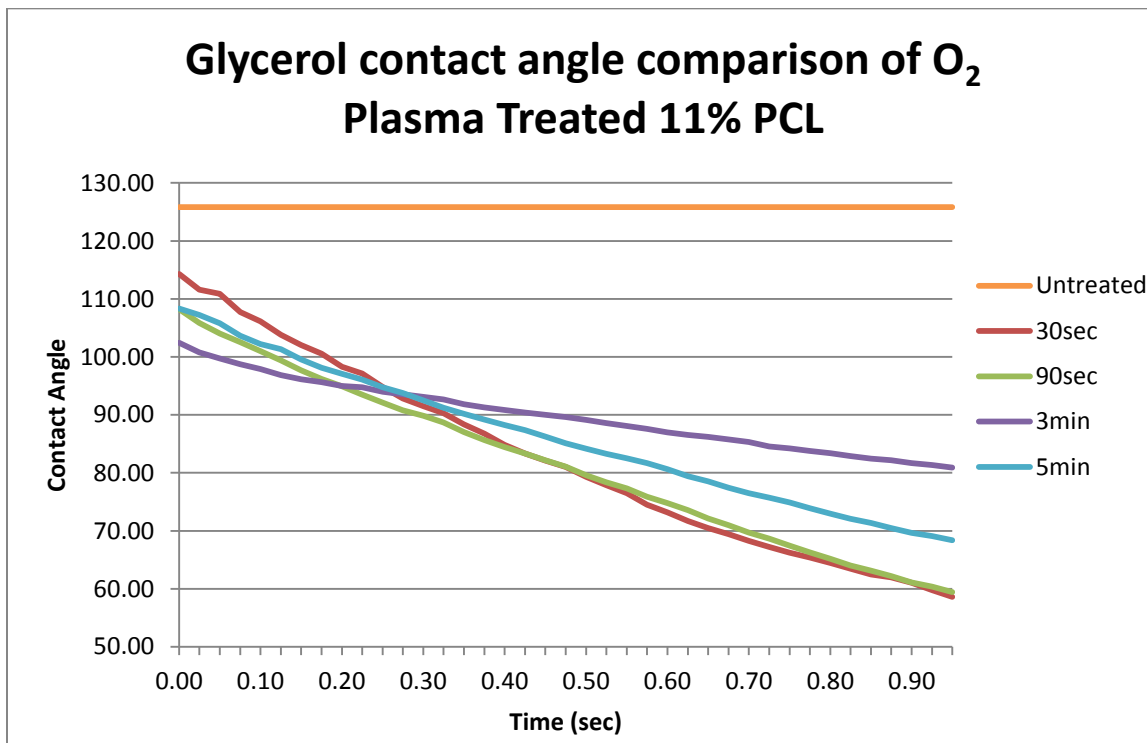


Fig. 5.6. Glycerol Contact Testing results for 11% PCL scaffolds treated with oxygen plasma for varying lengths of time

This data (**Fig. 5.6**) presents an interesting observation; the 3 and 5 min treatment of PCL scaffolds produced notably improved water contact angle results relative to the untreated sample, though the 30 and 90 s treated samples displayed the best results. It seems that the length of plasma treatment does not linearly correlate to induced hydrophilicity of the scaffolds. This sheds light on an important aspect of the production and analysis of polymer scaffolds and the optimal treatment and production parameters for maximal biocompatibility.

6. CELL GROWTH ON ELECTROSPUN SCAFFOLDS

In this experiment, we intended to determine whether the electrospun PCL nanofiber scaffolds could provide adequate niches for cells to grow. For this purpose we used NIH 3T3, a well characterized murine fibroblast cell line, as a model cell line. The electrospun PCL nanofiber scaffolds were treated with oxygen plasma for various lengths of time to improve their hydrophilicity before seeding the cells. To determine the proliferation of cells on the scaffolds, we employed the alamarBlue assay. AlamarBlue (AbD Serotec) is an assay based on a blue dye, resazurin, that is not inherently fluorescent, but the reduction of resazurin in mitochondria produces resorufin which fluoresces and can then be analyzed and quantified with a microplate reader. The amount and rate of reduction is attributed to, and directly correlated to, the rate of metabolic activity in the medium. Thus, by including a standard testing percentage (10%) of resazurin with medium added to cell culture dishes we can monitor and record the relative number of cells and their proliferation rates. In order to establish cell seeding levels that would provide adequate growth potential and give us baseline results we conducted a cell concentration proliferation assay. Growth rates for 4 different seeding densities were analyzed and results are shown in **Fig. 6.1**. These results indicate that a seeding density of 5×10^5 cells/ml is too high, leading to crowding and growth reduction over time. Based on these results we chose to seed 10000 cells into our scaffolds, exhibiting an effective 1.8×10^5 cells/ml. This would allow for growth on the scaffold's increased surface area while allowing significant room for growth and readings in our AlamarBlue assay over several days.

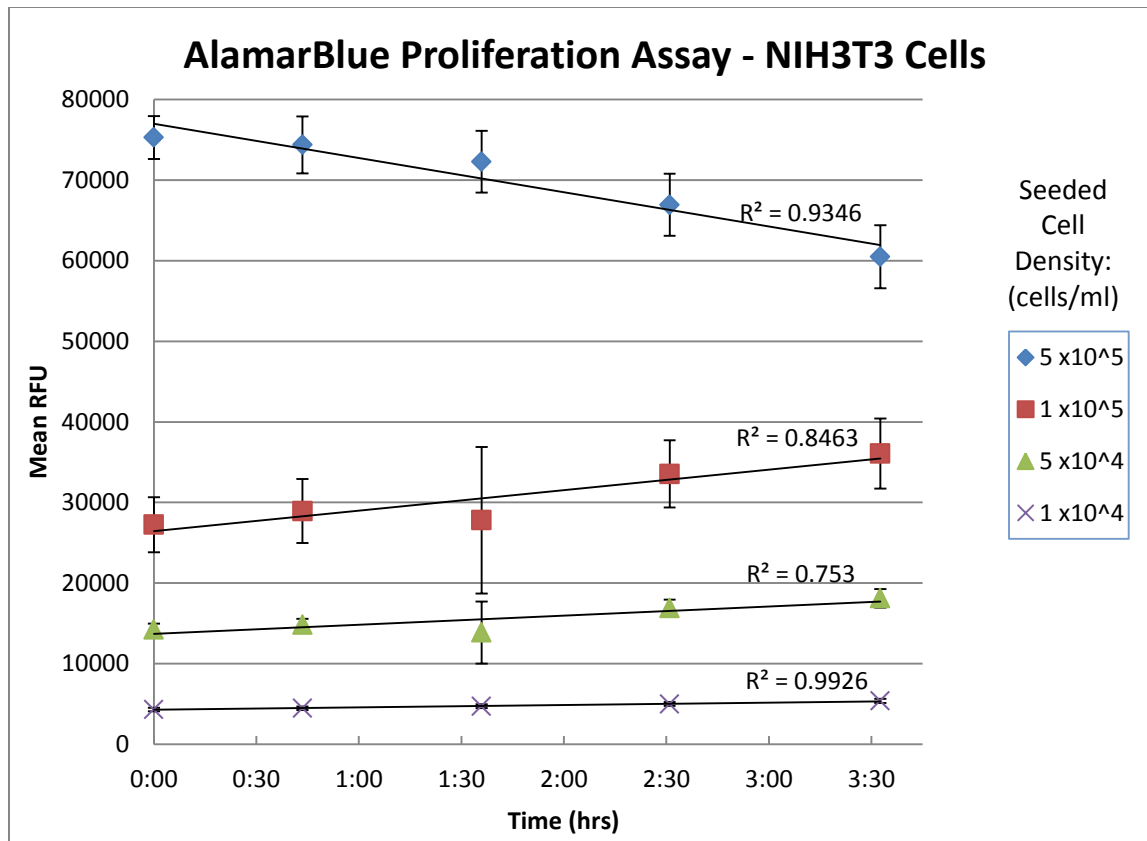


Fig. 6.1. AlamarBlue Cell Density Proliferation Assay. Four different cell densities were seeded and analyzed over a period of time to determine appropriate seeding density. The results indicate that a density of 5×10^5 is too high, leading to crowding and exhibiting a reduction of growth over time.

Taking as much care and precision as possible in distributing cell numbers amongst the different wells and amongst the different treated scaffolds we can propose that changes in metabolic activity and their activity relative to other wells signify the cells' ability to grow and proliferate on the scaffolds. Studies have shown alamarBlue to be nontoxic to cells[41] and so the addition of the dye should not exhibit any substantial effect on cell growth. We did, however, design our experiment to minimize the amount of incubation time with the dye in the medium, and performed daily medium exchanges to keep the cells growing in a stable and consistent condition.

The cells were seeded by carefully depositing droplets of cell solution (25 μ L) onto the center of the scaffolds, which were placed into 24 well ultra-low attachment plates. The use of ultra-low attachment plates (Costar ULA 3473) ensured that the cells' only attachment point was the scaffold, preventing additional variability in our results.

Our experimental timeline involved the addition of 10% alamarBlue after 20 h incubation in the fresh medium, followed by 4 h incubation to allow for metabolism of the dye and conversion of resazurin to the fluorescent resorufin. A sample of the medium from each well was then placed in a 96 well plate for fluorescence analysis in a microplate reader, and the remainder of the cell culture medium was carefully withdrawn and replaced with fresh cell culture medium (without alamarBlue). This 24 h cycle allowed for minimum exposure of the cells to the dye while keeping a consistent exposure time.

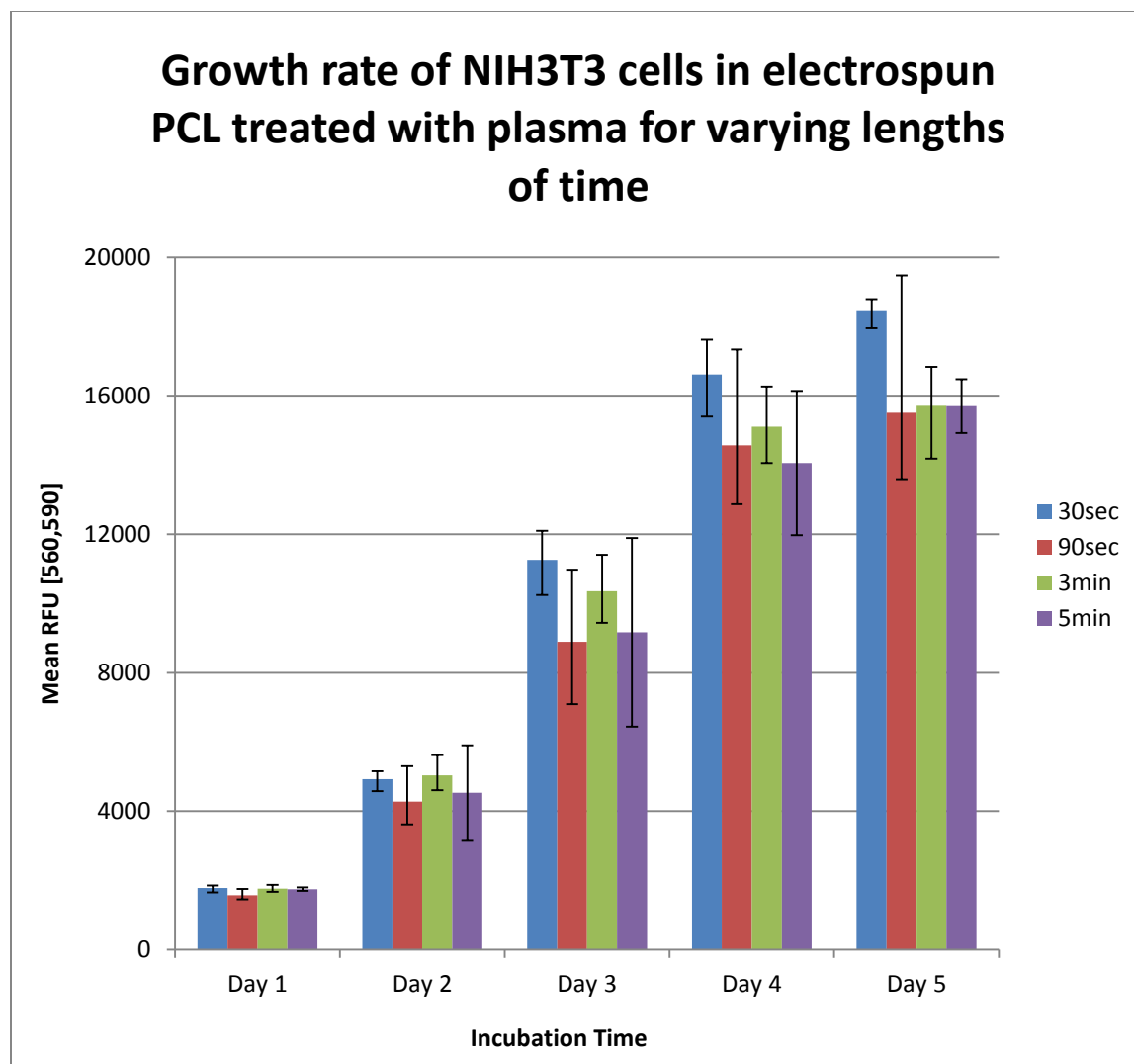


Fig. 6.2. Cell proliferation and growth rate assay. Daily growth rate as measured by fluorescence after 4 h incubation with alamarBlue. Following 20 h of incubation with cell culture medium, 10% alamarBlue was added to the medium and allowed to incubate for 4 h. This chart shows the results of fluorescent microplate readings following that incubation time on 5 consecutive days. Medium was exchanged immediately following the reading and the process was repeated 20 hours later. Error bars indicate maximum and minimum values.

Based on the data collected from this assay (**Fig. 6.2**), we can postulate that the 30 s plasma treatment time exhibits the most favorable growth environment for these cells in an 11% PCL electrospun scaffold, though the error bars indicate a lack of statistical significance. Proliferation rates for the remainder of the treatment samples showed similar growth patterns to each other,

but lower than that of the 30 second sample. As shown in **Fig. 5.6** all of the plasma treatment times showed a marked improvement in hydrophilicity, and during our experiments we had no problems with hydrophobicity in any of the treated samples. The untreated sample was incapable of accepting any medium or cells whatsoever due to its hydrophobicity (observed in the water contact angle testing) and thus was not included in the experiment. Further analysis of the growth data shows what would appear to be a reduction of growth on Day 5, with the chart beginning to level off. This can be due to several factors including a saturation of the growth surface area of the scaffolds, or a complete metabolism of 100% of the alamarBlue dye placed in the solution (which would explain a plateau effect, as the fluorescent material which can be produced is limited by the initial amount of dye added to the medium).

7. FUTURE WORKS

This study lays the groundwork for a variety of future projects. The electrospinning system developed and parameters optimized through this work allow for fabricating various electrospun nanofiber scaffolds with desired physiochemical properties. The finely tuned scaffolds can be used to direct stem cell differentiation in 3 D environments that mimic *in vivo* microenvironments required for cell-cell and cell-ECM interaction. In this work, we demonstrated the feasibility of growing cells within electrospun nanofiber scaffolds modified through oxygen plasma treatment. Although this work is very preliminary, it does lay out foundation for further exploring the proliferation and directed differentiation of stem cells within these nanofiber scaffolds. A future project could be designed to compare a variety of biocompatible polymer scaffolds with similar fiber size and morphology against each other. This could provide a direct material comparison so long as the other scaffolds have undergone a similar amount of specific investigation. Further experimentation could also be done on the effects of differing polymer concentrations on cell growth.

The data accumulated from plasma treatment allows for further investigation into individual treatment parameters for biocompatible polymer scaffolds while having set a baseline for expectations of results achieved over specific lengths of time. In this experiment we utilized the most favorable power, pressure, and flow parameters from previous works but did not take time to break down the effects of each of these individual settings on our induced hydrophilicity and tensile strength.

Finally, and perhaps most notably, future work could include the study of a variety of different cell types on this specifically designed scaffold. The purpose and goal of this scaffold was to provide a suitable and facilitative scaffold for cell growth, and it would be insightful to see the growth potential and activity of several cell types and cell lines. Stem cell in particular would be good candidates for further studies in these scaffolds as the added structure might promote improved cell-cell interaction and signaling, potentially leading to increased colony growth and health. The scaffold itself also provides a robust framework for transporting and implanting cells without disrupting their in-vitro growth progression, reducing the additional stresses related to their re-attachment at the implant site.

References

1. Li W-J, Laurencin CT, Caterson EJ, Tuan RS, Ko FK. Electrospun nanofibrous structure: a novel scaffold for tissue engineering. *Journal of biomedical materials research* [Internet]. 2002 Jun 15;60(4):613–21. Available from: <http://www.ncbi.nlm.nih.gov/pubmed/11948520>
2. Gilbert W. De Magnete [Internet]. London: Peter Short; 1628. Available from: <http://www.gutenberg.org/ebooks/33810>
3. Zeleny J. The electrical discharge from liquid points, and a hydrostatic method of measuring the electric intensity at their surfaces. *Physical Review* [Internet]. 1914 [cited 2011 Mar 28];3(2):69. Available from: http://prola.aps.org/abstract/PR/v3/i2/p69_1
4. Formhals A. Process and apparatus for preparing artificial threads: US, 1975504 [Internet]. 1934 [cited 2011 Oct 8]; Available from: <http://scholar.google.com/scholar?hl=en&btnG=Search&q=intitle:Process+and+Apparatu+s+for+preparing+artificial+threads#1>
5. Taylor G. Disintegration of Water Drops in an Electric Field. *Proceedings of the Royal Society A Mathematical Physical and Engineering Sciences* [Internet]. 1964;280(1382):383–97. Available from: <http://rspa.royalsocietypublishing.org/cgi/doi/10.1098/rspa.1964.0151>
6. Doshi J, Reneker DH. Electrospinning process and applications of electrospun fibers. *Journal of electrostatics* [Internet]. 1995 [cited 2011 Oct 8];35(2-3):151–60. Available from: <http://www.sciencedirect.com/science/article/pii/0304388695000418>
7. Li D, Xia Y. Electrospinning of Nanofibers: Reinventing the Wheel? *Advanced Materials* [Internet]. 2004 Jul [cited 2010 Jul 30];16(14):1151–70. Available from: <http://doi.wiley.com/10.1002/adma.200400719>
8. Huang L, Nagapudi K, P. Apkarian R, Chaikof EL. Engineered collagen–PEO nanofibers and fabrics. *Journal of Biomaterials Science, Polymer Edition* [Internet]. 2001 Oct;12(9):979–93. Available from: <http://www.catchword.com/cgi-bin/cgi?body=linker&ini=xref&reqdoi=10.1163/156856201753252516>
9. Matthews J a, Wnek GE, Simpson DG, Bowlin GL. Electrospinning of collagen nanofibers. *Biomacromolecules* [Internet]. 2002;3(2):232–8. Available from: <http://www.ncbi.nlm.nih.gov/pubmed/11888306>
10. Szentivanyi a., Assmann U, Schuster R, Glasmacher B. Production of biohybrid protein/PEO scaffolds by electrospinning. *Materialwissenschaft und Werkstofftechnik* [Internet]. 2009 Jan [cited 2010 Dec 8];40(1-2):65–72. Available from: <http://doi.wiley.com/10.1002/mawe.200800376>

11. Chen Z, Mo X, Qing F. Electrospinning of collagen–chitosan complex. *Materials Letters* [Internet]. 2007 Jun [cited 2010 Nov 7];61(16):3490–4. Available from: <http://linkinghub.elsevier.com/retrieve/pii/S0167577X06014170>
12. Zhong S, Teo WE, Zhu X, Beuerman RW, Ramakrishna S, Yue L, et al. An aligned nanofibrous collagen scaffold by electrospinning and its effects on in vitro fibroblast culture. *Journal of Biomedical Materials Research Part A*. 2006;
13. Buttafoco L, Kolkman NG, Engbers-Buijtenhuijs P, Poot a a, Dijkstra PJ, Vermes I, et al. Electrospinning of collagen and elastin for tissue engineering applications. *Biomaterials* [Internet]. 2006 Feb;27(5):724–34. Available from: <http://www.ncbi.nlm.nih.gov/pubmed/16111744>
14. Lannutti J, Reneker D, Ma T, Tomasko D, Farson D. Electrospinning for tissue engineering scaffolds. *Materials Science and Engineering: C* [Internet]. 2007 Apr [cited 2010 Oct 12];27(3):504–9. Available from: <http://linkinghub.elsevier.com/retrieve/pii/S0928493106001421>
15. Eng JT, Med R, Sant S, Hwang CM, Lee S-hoon, Khademhosseini A. Hybrid PGS – PCL microfibrinous scaffolds with improved mechanical and biological properties. *Scanning Electron Microscopy*. 2010;
16. Shih Y-RV, Chen C-N, Tsai S-W, Wang YJ, Lee OK. Growth of mesenchymal stem cells on electrospun type I collagen nanofibers. *Stem cells (Dayton, Ohio)* [Internet]. 2006 Nov;24(11):2391–7. Available from: <http://www.ncbi.nlm.nih.gov/pubmed/17071856>
17. Powell HM, Boyce ST. Engineered human skin fabricated using electrospun collagen-PCL blends: morphogenesis and mechanical properties. [Internet]. *Tissue engineering. Part A*. 2009 Aug;15(8):2177–87. Available from: <http://www.ncbi.nlm.nih.gov/pubmed/19231973>
18. Lee SJ, Liu J, Oh SH, Soker S, Atala A, Yoo JJ. Development of a composite vascular scaffolding system that withstands physiological vascular conditions. *Biomaterials* [Internet]. 2008 Jul;29(19):2891–8. Available from: <http://www.ncbi.nlm.nih.gov/pubmed/18400292>
19. Serrano MC, Pagani R, Vallet-Regí M, Peña J, Rámila A, Izquierdo I, et al. In vitro biocompatibility assessment of poly(epsilon-caprolactone) films using L929 mouse fibroblasts. *Biomaterials* [Internet]. 2004 Nov [cited 2010 Dec 8];25(25):5603–11. Available from: <http://www.ncbi.nlm.nih.gov/pubmed/15159076>
20. Pritchard CD, Arnér KM, Neal R a, Neeley WL, Bojo P, Bachelder E, et al. The use of surface modified poly(glycerol-co-sebacic acid) in retinal transplantation. *Biomaterials* [Internet]. 2010 Mar [cited 2010 Aug 10];31(8):2153–62. Available from: <http://www.ncbi.nlm.nih.gov/pubmed/19962754>

21. Reichert JC, Heymer a, Berner a, Eulert J, Nöth U. Fabrication of polycaprolactone collagen hydrogel constructs seeded with mesenchymal stem cells for bone regeneration. *Biomedical materials* (Bristol, England) [Internet]. 2009 Dec [cited 2010 Aug 9];4(6):065001. Available from: <http://www.ncbi.nlm.nih.gov/pubmed/19837997>
22. Coombes a. G a., Rizzi SC, Williamson M, Barralet JE, Downes S, Wallace W a. Precipitation casting of polycaprolactone for applications in tissue engineering and drug delivery. *Biomaterials* [Internet]. 2004 Jan [cited 2011 Jun 8];25(2):315–25. Available from: <http://linkinghub.elsevier.com/retrieve/pii/S0142961203005350>
23. Lowery JL, Datta N, Rutledge GC. Effect of fiber diameter, pore size and seeding method on growth of human dermal fibroblasts in electrospun poly(epsilon-caprolactone) fibrous mats. *Biomaterials* [Internet]. 2010 Jan;31(3):491–504. Available from: <http://www.ncbi.nlm.nih.gov/pubmed/19822363>
24. Yildirim E, Besunder R, Pappas D, Allen F. Accelerated differentiation of osteoblast cells on polycaprolactone scaffolds driven by a combined effect of protein coating and plasma modification. *Biofabrication* 2 [Internet]. 2010 [cited 2012 Feb 5];014109. Available from: <http://iopscience.iop.org/1758-5090/2/1/014109>
25. Duan Y, Wang Z, Yan W, Wang S, Zhang S, Jia J. Preparation of collagen-coated electrospun nanofibers by remote plasma treatment and their biological properties. *Journal of biomaterials science. Polymer edition* [Internet]. 2007 Jan;18(9):1153–64. Available from: <http://www.ncbi.nlm.nih.gov/pubmed/17931505>
26. Martins A, Pinho ED, Faria S, Pashkuleva I, Marques AP, Reis RL, et al. Surface modification of electrospun polycaprolactone nanofiber meshes by plasma treatment to enhance biological performance. *Small* (Weinheim an der Bergstrasse, Germany) [Internet]. 2009 May;5(10):1195–206. Available from: <http://www.ncbi.nlm.nih.gov/pubmed/19242938>
27. Oyane A, Uchida M, Yokoyama Y, Choong C, Triffitt J, Ito A. Simple surface modification of poly(epsilon-caprolactone) to induce its apatite-forming ability. *Journal of biomedical materials research. Part A* [Internet]. 2005 Oct [cited 2010 Dec 8];75(1):138–45. Available from: <http://www.ncbi.nlm.nih.gov/pubmed/16044403>
28. Mitchell SB, Sanders JE. A unique device for controlled electrospinning. *Journal of Biomedical Materials Research Part A*. 2006;(August 2005).
29. Theron S. Experimental investigation of the governing parameters in the electrospinning of polymer solutions. *Polymer* [Internet]. 2004;45(6):2017–30. Available from: <http://linkinghub.elsevier.com/retrieve/pii/S0032386104000485>
30. Reneker DH, Yarin AL. Electrospinning jets and polymer nanofibers. *Polymer* [Internet]. 2008;49(10):2387–425. Available from: <http://linkinghub.elsevier.com/retrieve/pii/S0032386108001407>

31. Han D, Gouma P-I. Electrospun bioscaffolds that mimic the topology of extracellular matrix. *Nanomedicine : nanotechnology, biology, and medicine* [Internet]. 2006 Mar [cited 2010 Oct 10];2(1):37–41. Available from: <http://www.ncbi.nlm.nih.gov/pubmed/17292114>
32. Zhang Y, He Y, Bharadwaj S, Hammam N, Carnagey K, Myers R, et al. Tissue-specific extracellular matrix coatings for the promotion of cell proliferation and maintenance of cell phenotype. *Biomaterials* [Internet]. 2009 Aug;30(23-24):4021–8. Available from: <http://www.ncbi.nlm.nih.gov/pubmed/19410290>
33. Mie M, Mizushima Y, Kobatake E. Novel extracellular matrix for cell sheet recovery using genetically engineered elastin-like protein. *Journal of biomedical materials research. Part B, Applied biomaterials* [Internet]. 2008 Jul [cited 2010 Dec 8];86(1):283–90. Available from: <http://www.ncbi.nlm.nih.gov/pubmed/18161837>
34. Gruber HE, Mauerhan D, Chow Y, Ingram J a, Norton HJ, Hanley EN, et al. Three-dimensional culture of human meniscal cells: extracellular matrix and proteoglycan production. *BMC biotechnology* [Internet]. 2008 Jan;8:54. Available from: <http://www.ncbi.nlm.nih.gov/pubmed/18582376>
35. Deister C, Aljabari S, Schmidt CE. Effects of collagen 1, fibronectin, laminin and hyaluronic acid concentration in multi-component gels on neurite extension. *Journal of biomaterials science. Polymer edition* [Internet]. 2007 Jan;18(8):983–97. Available from: <http://www.ncbi.nlm.nih.gov/pubmed/17705994>
36. Zhu Y, Chan-Park MB. Density quantification of collagen grafted on biodegradable polyester: its application to esophageal smooth muscle cell. *Analytical biochemistry* [Internet]. 2007 Apr 1 [cited 2010 Nov 19];363(1):119–27. Available from: <http://www.ncbi.nlm.nih.gov/pubmed/17292321>
37. Sisson K, Zhang C, Farach-Carson MC, Chase DB, Rabolt JF. Evaluation of Cross-Linking Methods for Electrospun Gelatin on Cell Growth and Viability. *Biomacromolecules* [Internet]. 2009 May;10(7). Available from: <http://www.ncbi.nlm.nih.gov/pubmed/19456101>
38. Han B, Jaurequi J, Tang BW, Nimni ME. Proanthocyanidin: a natural crosslinking reagent for stabilizing collagen matrices. *Journal of biomedical materials research. Part A* [Internet]. 2003 Apr 1;65(1):118–24. Available from: <http://www.ncbi.nlm.nih.gov/pubmed/12635161>
39. Heydarkhan-Hagvall S, Schenke-Layland K, Dhanasopon AP, Rofail F, Smith H, Wu BM, et al. Three-dimensional electrospun ECM-based hybrid scaffolds for cardiovascular tissue engineering. *Biomaterials* [Internet]. 2008 Jul;29(19):2907–14. Available from: <http://www.ncbi.nlm.nih.gov/pubmed/18403012>

40. Kim S, Nimni ME, Yang Z, Han B. Chitosan/gelatin-based films crosslinked by proanthocyanidin. *Journal of biomedical materials research. Part B, Applied biomaterials* [Internet]. 2005 Nov [cited 2010 Dec 8];75(2):442–50. Available from: <http://www.ncbi.nlm.nih.gov/pubmed/16047322>
41. O'Brien J, Wilson I, Orton T, Pognan F. Investigation of the Alamar Blue (resazurin) fluorescent dye for the assessment of mammalian cell cytotoxicity. *European journal of biochemistry / FEBS* [Internet]. 2000 Sep;267(17):5421–6. Available from: <http://www.ncbi.nlm.nih.gov/pubmed/10951200>

APPENDIX

Methods and Materials:

1. Preparation of polymer solution:

- a. In a chemical fume hood mix 22.5 ml chloroform and 7.5 ml methanol into a sealable glass flask, forming a 3:1 mixture.
- b. Measure 3.3 g PCL (Sigma, ~70,000-90,000 mw, cat. no. 440744) and add to the solution.
- c. Seal the flask and place mixture in an orbital shaker for 2-5 h at 37⁰C to form a homogenous solution.
- d. Allow solution to cool to room temperature for 60 min.
- e. Fit a 14G needle onto a syringe (BD 309585, Polypropylene, Luer-Lok) and (in a chemical fume hood) slowly draw the desired amount (1.5 ml) into the syringe, being careful to avoid adding bubbles to the solution within the syringe.
- f. Set the needle on its end (tip facing up) and allow it to sit for 10-15 min to allow bubbles to seep out.
- g. Remove the 14G needle and replace it with an 18G needle (Howard Electronics JG18-1.5, ID=0.038", OD=0.049")
- h. Remove the remainder of air in the syringe without any solution reaching the needle tip.

2. Electrospinning:

- a. Place the polycarbonate enclosure into a chemical fume hood.

- b. Attach the charge distribution plate to the positive lead from the power supply (Spellman CZE 1000R) *via* the screw and washer in the plate collar.
- c. Mount the syringe into the horizontal syringe pump (KD Scientific KDS-101) and fit the charge distribution plate onto the needle - leaving 4 mm between the face of the plate and the tip of the needle. Secure the plate to the needle via the set-screw on the plate collar.
- d. Mount the grounded collector plate (6" square, 1/8" aluminum) 20 cm from the tip of the needle when the syringe is mounted to the syringe pump. Center the plate based on the needle location.
- e. With double sided tape, mount a 7" x 7" piece of wax paper onto the face of the collector plate. This will facilitate sample removal from the collector without disturbing the scaffold.
- f. Set the power supply to 30 kV (positive) and leave off.
- g. Prime the needle (80 μ L solution) without ejecting the solution, and set the syringe pump to 1.2 ml with a rate of 95 μ L / min.
- h. Turn the power supply on (door switch will keep it inactive) and start the syringe pump. Hold the door from closing while carefully observing the tip of the needle. As soon as any solution is visible immediately close the door – inactivating the kill-switch and turning on the voltage.
- i. Monitor the stream throughout the electrospinning process to ensure consistent fiber formation and absence of visible droplet formation on the needle tip.
- j. When the syringe pump stops (1.2 ml) immediately open the door, inactivating the power supply.

- k. Leave the door slightly open and turn on the fume hood for 1-2 min to remove the fumes within the enclosure.
- l. Carefully remove the wax paper containing the scaffold from the collector plate, taking care not to fold or wrinkle the sample.
- m. Place the paper with sample immediately into a sterile enclosure.
- n. Repeat as necessary.

3. Plasma Treatment:

- a. Remove the scaffold from the wax paper by gently separating it at its edge.
- b. Carefully place the scaffold on an RIE wafer (metal) and tape the edges as necessary using RIE-safe tape. Be sure to contact as little of the scaffold as possible with the tape, as those areas will be discarded following the plasma treatment process.
- c. Follow the general protocols to insert the wafer and sample into the RIE (Plasma Therm SLR 720). Set the treatment parameters as follows: 20 sccm oxygen, 100 mTorr, 30W, 13.56 MHz.
- d. Run the treatment for the desired length of time (30 s, 90 s, 3 min, and 5 min).
- e. Repeat as required for each sample for the desired length of time (2 of each).
- f. Cut the sample from the wafer by tracing the inner edges of the tape, leaving the taped portions of the scaffold on the wafer. Place the sample in a sterile container, and remove the tape from the wafer.

4. Scaffold preparation:

- a. Cut samples on a sterile polypropylene cutting board with a rubber mallet and 12 mm sterile round punch.
- b. Sterilize under UV for 30 min on each side, making sure to keep track of which side is up. Handle carefully when flipping the scaffold with tweezers, gripping only the very edge to minimize disruption of the fibers.
- c. Place samples in a 24 well ULA dish (Costar ULA 24 well, cat. no.3473) and rinse 3 times with 500 μ l DMEM.
- d. Rinse samples 1x with 500 μ l cell growth medium, aspirate.
- e. Add 750 μ l of growth medium and incubate overnight at 37°C, 5% CO₂.

5. Cell preparation from T25 flask:

- a. Rinse 2-3x with PBS
- b. Add 1 ml trypsin and incubate for 3-5 min
- c. Add medium, rinse surface, and collect in a 15 ml corning tube
- d. Agitate medium to evenly distribute cells and break down clumps
- e. Immediately remove 25 μ l for cell count
- f. Centrifuge @ 300 x g for 5 min @ room temperature
- g. Conduct cell count during this time
- h. Calculate number of cells present in the 15 ml corning tube and desired dilution for 10⁴ cells / 25 μ l of medium (400,000 cells / ml)
- i. Aspirate medium until 2-4 ml are left
- j. Aspirate remaining medium with a 5 ml pipet and pipettman to ensure no loss of cells (invalidating cell count)

- k. Add calculated amount of medium to achieve proper cell count

6. Cell seeding:

- a. Rinse scaffolds 1x with 500 μ l medium
- b. Completely aspirate medium, and add 25 μ l of cell suspension drop-wise to the center of each scaffold.
- c. Incubate for 1 h to allow cells to attach.
- d. Carefully add 425 μ l medium and incubate overnight

7. AlamarBlue Assay:

- a. Following 20 h incubation, carefully add 50 μ l alamarBlue to the samples, producing a 10% alamarBlue solution.
- b. Incubate for 4 h (37°C, 5% CO₂).
- c. Gently pipet 50 μ l in and out 2 x to carefully stir the cell solution.
- d. Remove 50 μ l of the cell solution and place in a 96 well plate for analysis.
- e. Slowly and carefully aspirate the remainder of the cell solution and add 450 μ l of fresh cell medium. Incubate 20 h and repeat process for each day.
- f. Immediate take the 50 μ l samples to a microplate reader (BioTek Synergy Ht) and run a fluorescence assay to determine amount of reduced resorufin present. This will indicate the metabolic rates of the cells in the medium over 4 hours, providing an indication of cell growth and proliferation.

8. SEM protocol:

- a. Obtain SEM bullets and place a small section of double sided carbon tape on top of the bullet.
- b. Mount a small sample of the scaffold to the double sided tape without damaging or compressing the sample.
- c. Use a sputter coating machine to coat the surface with gold nanoparticles. (Anatech Hummer VI-A sputter coater, 150 s, 15 mA, 18 mTorr)
- d. Mount the bullets in a suitable carrier and follow local protocol to place them into the SEM. (JEOL JSM-6335F)
- e. Observe at 5 kV

9. Contact Angle Testing:

- a. Mount sample carefully by placing it on a microscope slide using double-sided tape on only the edges. Using this tape beneath the sample may interfere with absorption.
- b. Place the slide on the platform of the contact angle testing instrument (Digital Physics - OCA 15) and center the sample beneath the needle tip.
- c. Select an appropriate droplet size (0.5 μ l) and eject it while capturing the high speed video.
- d. Use the software to analyze the droplet contact angles recorded over a period of time.

10. Tensile testing:

- a. Select a sample large enough to accommodate an evenly thick 50 x 50 mm square section.

- b. Print the template provided in Fig. 5.1b to the correct noted scale.
- c. Cut out the central 30 x 30 mm square section
- d. Place double-sided tape along the left and right 10 x 10 mm sections of the remaining square.
- e. Carefully place the remaining hollow square onto the center of the previously prepared sample. Note that the double-sided tape should be facing down onto the sample. Once this has been placed on the sample its location cannot be adjusted without destroying the sample.
- f. Using a straight edge as a guide – cut with a scalpel from one end of the square to the other – creating three 10 x 50 mm strips. Each end of the strip should be covered by a 10 x 10 mm piece of paper attached with the double-sided tape, with a 30 x 10 mm section between them.
- g. Place the mounting tabs (10 x 10 mm) into the mounting clamps for tensile testing (Instron 3365, 500N load cell). Leave only the 10 x 30 mm gauge length exposed between the clamps.
- h. Run the Instron at 15 mm/min while collecting data every 50 ms until the material fails.

Vitae

Publications:

Jin S, Yao H, Haukas A, Ye K. Porous Membrane Substrates Offer Better Tissue Niches to Enhance the Wnt Signaling and Promote Human Embryonic Stem Cell Growth and Differentiation. Tissue Engineering. [In-Press 2011]

Poster Presentations:

“Differentiation of Human iPS Cells Into Pancreatic β -cells in a 3-D Scaffold”, Haukas A, BMES 2009